

Combining Different Hydrogen-Bonding Motifs To Self-Assemble Interwoven Superstructures**

Peter R. Ashton, Matthew C. T. Fyfe, Sarah K. Hickingbottom, Stephan Menzer, J. Fraser Stoddart,* Andrew J. P. White, and David J. Williams*

Abstract: A series of carboxyl-substituted dibenzylammonium salts have been cocrystallized with the macrocyclic polyethers dibenzo[24]crown-8 (DB24C8) and bis-*p*-phenylene[34]crown-10 (BPP34C10) to effect the noncovalent syntheses of a wide range of interwoven superstructures in the solid state. In all cases, the dibenzylammonium cations thread through the cavities of the macrocyclic polyethers—primarily as a result of N⁺–H···O hydrogen bonds, with occasional secondary stabilization from C–H···O and aryl–aryl interactions—to form pseudorotaxane complexes possessing supplementary recognition sites (specifically, carboxyl groups) for further intercomplex association through hydrogen bonding. One unit of each of the dibenzylammonium cations threads through the DB24C8 macrocycle to make single-stranded, carboxyl-contain-

ing [2]pseudorotaxanes that interact further with one another to produce novel supramolecular architectures as a result of hydrogen bonding between their carboxyl groups (the carboxyl dimer supramolecular synthon), or between carboxyl groups and polyether oxygen atoms. Elaborate architectures, such as side-/main-chain pseudopolyrotaxanes and a daisy-chain-like supramolecular array, were thus synthesized noncovalently. BPP34C10 can accommodate two cations within its macrocyclic interior to form carboxyl-containing [3]pseudorotaxanes in which BPP34C10 acts as a girdle that helps to control the spatial

orientation of the carboxylic acid-containing recognition sites for additional intersupramolecular association through the carboxyl dimer. PF₆⁻ anions were also found to play a role in the self-assembly processes. When the anions interact with the [3]pseudorotaxanes, these recognition sites are oriented in the same direction. This leads to the formation of doubly-encircled multicomponent supermolecules when BPP34C10 is cocrystallized with dibenzylammonium cations bearing only one carboxyl substituent. On the other hand, when BPP34C10 is cocrystallized with an isophthalic acid-substituted ammonium cation, there is no evidence of any anion assistance to self-assembly; the isophthalic acid units are aligned in opposite directions, creating an interwoven supramolecular cross-linked polymer.

Keywords: crystal engineering · hydrogen bonds · interwoven systems · self-assembly · supramolecular chemistry

Introduction

Scientists pursuing research on the chemistry of the noncovalent bond—that is, supramolecular chemistry^[1]—are constantly discovering new recognition motifs that allow them to synthesize specific supramolecular architectures noncovalently with remarkable control and precision.^[2] We believe that the controlled supramolecular synthesis^[3] of functioning, organized nanostructures, the likes of which have been identified previously only in nature, will become possible in the near future. On account of its directionality and its ability to discriminate between various recognition

motifs, the hydrogen bond has been harnessed for the noncovalent synthesis of some remarkable superstructures,^[4] ranging from discrete, multicomponent supermolecules^[5] to infinite, polymeric supramolecular arrays.^[6] We have recently reported^[7] the discovery of practicable, and remarkably simple, self-assembling supramolecular systems that utilize hydrogen bonds as their principal noncovalent adhesive. Secondary dialkylammonium cations, such as the dibenzylammonium ion (**1**⁺), self-assemble^[8] with macrocyclic polyethers to form multicomponent pseudorotaxanes (Figure 1),^[9] the stoichiometry of which may be controlled accurately. Pseudorotaxanes possessing from two to five organic compo-

[*] Prof. J. F. Stoddart,^[+] Dr. M. C. T. Fyfe, P. R. Ashton, S. K. Hickingbottom
School of Chemistry, University of Birmingham
Edgbaston, Birmingham B15 2TT (UK)
Prof. D. J. Williams, Dr. S. Menzer, Dr. A. J. P. White
Department of Chemistry, Imperial College
South Kensington, London SW7 2AY (UK)
Fax: (+ 44) 171-594-5804

[+] Current address: Department of Chemistry and Biochemistry
University of California, Los Angeles
405 Hilgard Avenue, Los Angeles CA 90095-1569 (USA)
Fax: (+ 1) 310-206-1843
E-mail: stoddart@chem.ucla.edu

[**] Molecular Meccano, Part 34. For Part 33, see: P. R. Ashton, I. Baxter, M. C. T. Fyfe, F. M. Raymo, N. Spencer, J. F. Stoddart, A. J. P. White, D. J. Williams, *J. Am. Chem. Soc.* **1998**, *220*, 2297.

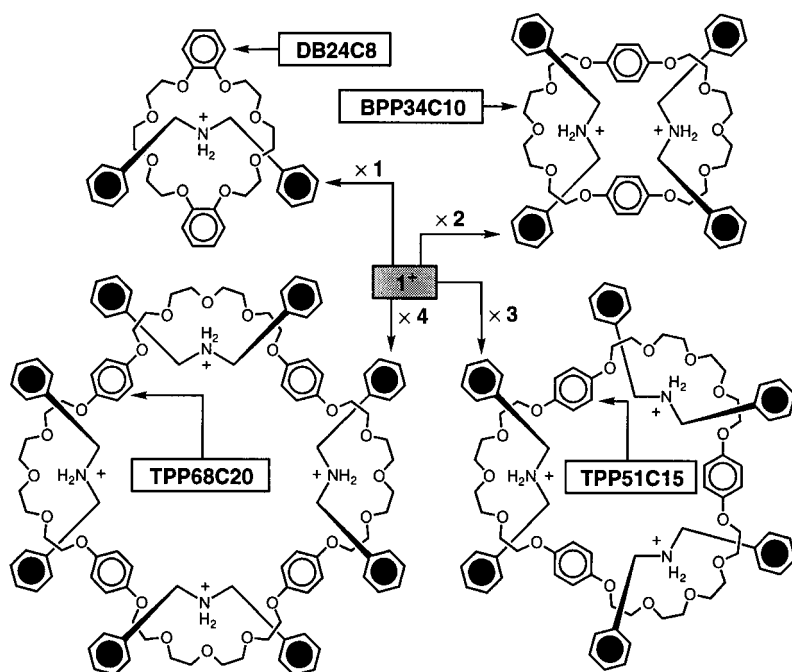


Figure 1. The wide range of multicomponent pseudorotaxane supermolecules that can be self-assembled from the dibenzylammonium cation (1^+) and various macrocyclic polyethers.

nents may be synthesized noncovalently, depending on the size of the internal cavity of the macrocyclic polyether. For instance, dibenzo[24]crown-8 (DB24C8) forms a 1:1 [2]pseudorotaxane complex with 1^+ in which the ammonium thread interpenetrates the macroring cavity by virtue of $N^+ - H \cdots O$ and $C-H \cdots O$ hydrogen bonds, supplemented by $\pi - \pi$ stacking interactions.^[7a, c, d] Moreover, the crown ether component can become ditopic (i.e., it can accommodate two ammonium centers within its interior) provided its two polyether loops are disassociated from one another, as in the case of bis-*p*-phenylene[34]crown-10 (BPP34C10), which forms a double-stranded [3]pseudorotaxane with 1^+ .^[7b-d] This paradigm can be extended even further:^[7f-g] the crown ethers tris-*p*-phenylene[51]crown-15 (TPP51C15) and tetrakis-*p*-phenylene[68]crown-20 (TPP68C20) can bind three and four 1^+ cations, respectively, within their macrocyclic cores, since they possess three and four separated polyether loops, each of which can form hydrogen bonds with the ammonium centers. Furthermore, on account of the expanded nature of their crown ether macrorings, the resultant [4]- and [5]pseudorotaxanes possess ammonium centers that are ideally predisposed to associate with anions by hydrogen bonding and anion-dipole interactions.

Another hydrogen bonding motif that has been studied extensively^[10] by supramolecular chemists is the carboxyl dimer supramolecular synthon. In particular, researchers interested in crystal engineering^[11] (the rational design of organized solid-state superstructures) have employed this recognition motif for the noncovalent synthesis of a wide range of supramolecular architectures. By way of illustration, crystal engineers have utilized the carboxylic dimer for the solid-state noncovalent synthesis of ribbon-like supramolecular arrays (Figure 2), such as is observed in the crystal structures of terephthalic acid^[12] and isophthalic acid.^[13]

Moreover, the placement of bulky alkyl substituents on the isophthalic acid moiety induces^[14] the production of a hexameric, hydrogen-bonded supramolecular macrocycle, thereby relieving unfavorable nonbonding interactions.

We conjectured that we could utilize the directional attributes of the hydrogen bond for the noncovalent syntheses of interwoven supramolecular architectures involving the aggregation/polymerization of pseudorotaxanes^[15,16] in the solid state. It seemed to us that interwoven superstructures could be synthesized noncovalently by combining both i) the threading of secondary dialkylammonium cations through crown ethers, and ii) the supramolecular dimerization of carboxyl groups. The threading motif would allow the creation of multicomponent pseudorotaxanes that would be endowed with pendant carboxyl groups for further noncovalent association to produce novel interwoven superstructures. Here, we report that carboxyl-containing, crown ether-dialkylammonium-based pseudorotaxanes (generated when the crown ethers DB24C8 and BPP34C10 complex with the carboxyl-substituted dibenzylammonium cations $2^+ - 6^+$, Figure 3) do indeed associate with one another to form unique interwoven supermolecules and supramolecular arrays in the solid state.^[17]

Results and Discussion

Molecular synthesis: The salts $2 \cdot PF_6 - 6 \cdot PF_6$, possessing both secondary ammonium centers for the formation of pseudorotaxanes with crown ethers, and carboxyl groups for the noncovalent association of these pseudorotaxanes, were readily obtained using the protocol outlined in Scheme 1. Condensation of the appropriate aldehydes and amines furnished aldimines that were subsequently reduced to the secondary amines **13**–**17** possessing appended benzoate or isophthalate moieties. Ultimately, each of these esters was converted into its corresponding salt $2 \cdot PF_6 - 6 \cdot PF_6$ by boiling

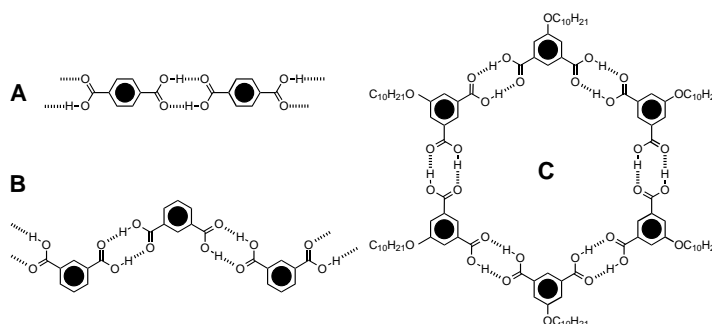


Figure 2. Examples of some of the supramolecular architectures that can be synthesized noncovalently, from various building blocks, with the carboxyl dimer supramolecular synthon. Tape-like supramolecular polymers from A) terephthalic acid and B) isophthalic acid. C) Hexameric supramolecular macrocycle from 5-decyloxyisophthalic acid.

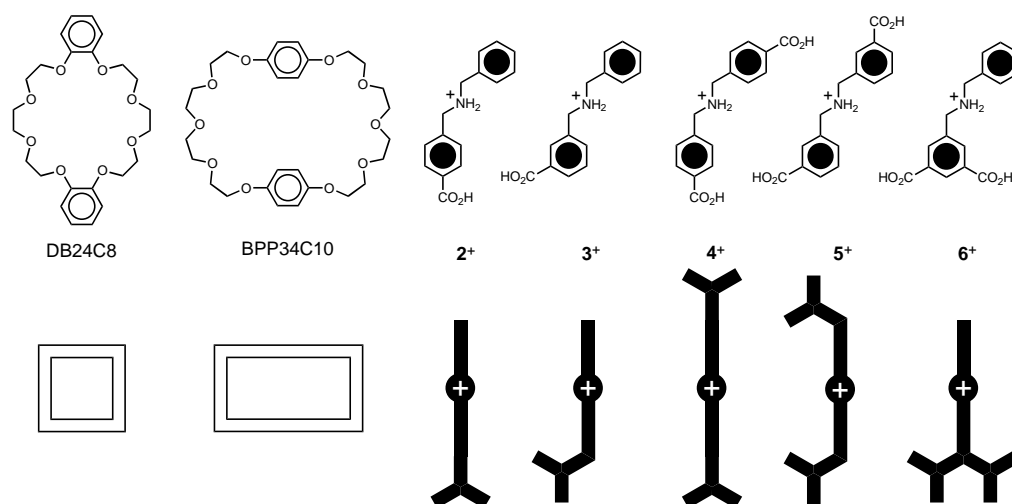


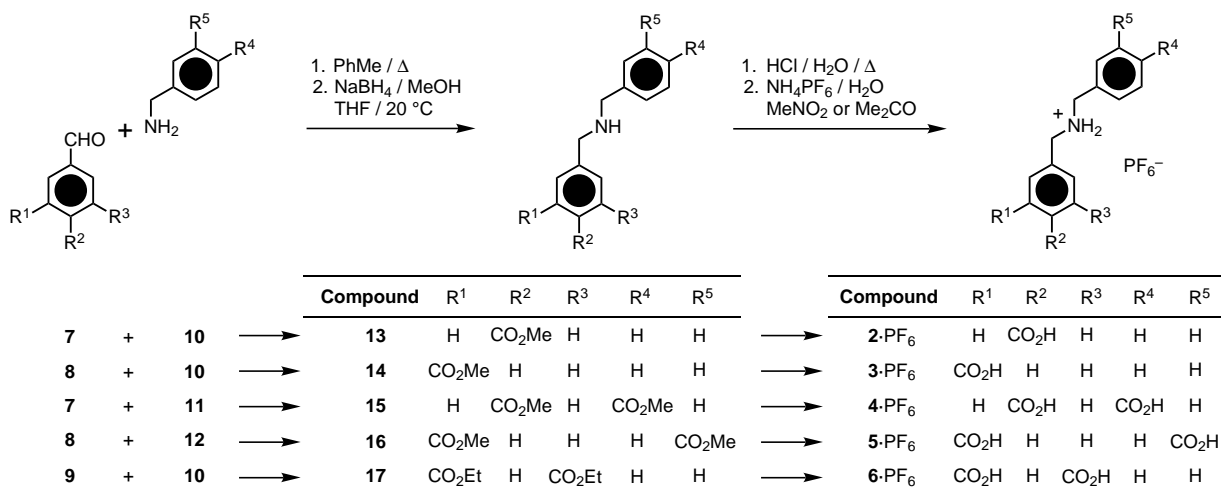
Figure 3. Chemical formulas and cartoon representations for the macrocyclic polyethers and carboxyl-substituted dibenzylammonium cations studied in this paper. Note that the aromatic rings are not represented, for the sake of clarity, in the cartoons exhibited in the ensuing figures.

with hydrochloric acid (to effect hydrolysis with concomitant protonation) followed by counterion exchange from chloride to hexafluorophosphate. With the exception of **9** and **12**, the aldehyde and amine precursors of the salts were either commercially available or were known compounds. The aldehyde **9** was prepared by oxidation of diethyl 5-bromomethylisophthalate^[18] with bis(tetrabutylammonium) dichromate,^[19] while the amine **12** was obtained by Fischer–Speier esterification of 3-carboxybenzylammonium chloride^[20] with MeOH. The crown ethers employed in the supramolecular syntheses (specifically DB24C8 and BPP34C10) were also obtained easily: DB24C8 is commercially available, while BPP34C10 can be readily prepared^[21] by a one-pot reaction of hydroquinone with tetraethylene glycol bisosylate.

Characterization of pseudorotaxanes in solution and the gas phase: In a similar manner to that of their unsubstituted congener **1**,^[7a–d] the carboxyl-substituted dibenzylammonium cations **2**⁺–**6**⁺ form pseudorotaxane complexes with DB24C8

and BPP34C10 in both solution and in the gas phase, as ascertained by ¹H NMR spectroscopy and liquid secondary ion mass spectrometry (LSIMS), respectively.

As anticipated from studies on the parent dibenzylammonium salt **1**·PF₆,^[7a, c, d] solutions of DB24C8 and the salts **2**·PF₆–**6**·PF₆ exhibit somewhat slow kinetic exchange with their complexes, since it is especially difficult for the aromatic rings of the cations to pass through the relatively small cavity of the DB24C8 macrocycle. In particular, this exchange is slow enough on the NMR time scale that the ¹H NMR spectra of equimolar solutions of DB24C8 and the salts display three sets of resonances for i) the uncomplexed crown ether, ii) the uncomplexed carboxyl-substituted dibenzylammonium salt, and iii) the 1:1 complex formed between these two species. The chemical shift data for the compounds and complexes are listed in Table 1, which shows that the proton resonances associated with the pseudorotaxane complexes are shifted quite dramatically from those in the uncomplexed crown ether and salt. Furthermore, the observation of signals



Scheme 1. Synthetic protocol employed for the preparation of the salts **2**·PF₆–**6**·PF₆. Compound **7**: methyl 4-formylbenzoate; **8**: methyl 3-formylbenzoate; **9**: diethyl 5-formylisophthalate; **10**: benzylamine; **11**: methyl 4-aminomethylbenzoate; **12**: methyl 3-aminomethylbenzoate.

associated with both the complex and its uncomplexed constituents permits facile single-point measurements of the [2]pseudorotaxanes' association constants (K_a),^[7a, c, d] from which their related free energies of complexation (ΔG°) can be derived (Table 2). The data reveal that the carboxyl-substituted ammonium cations **2**⁺–**6**⁺ form much stronger complexes with DB24C8 than does the unsubstituted cation **1**⁺, presumably as a direct consequence of i) resonance and inductive effects, which increase the acidity of both the benzylic methylene and NH_2^+ hydrogen atoms, and ii) the greater tendency of the π -electron-deficient $\text{Ar}(\text{CO}_2\text{H})_n$ rings of the cation to enter into aryl–aryl stacking interactions with the π -electron-rich catechol rings of the DB24C8 macrocycle. Moreover, it can be seen that, as a result of resonance effects on the hydrogen-bonding ability of the benzylic methylene moieties, ammonium cations bearing *p*-carboxy groups form stronger complexes with DB24C8 than the *m*-substituted congeners. In addition, it is evident that ammonium cations bearing two electron-withdrawing carboxyl substituents form stronger complexes than those bearing one, but that the strength of a complex is increased more spectacularly when the two carboxyl units are situated on the *same* aromatic ring. 1:1 Mixtures of DB24C8 and the salts **2**·PF₆–**6**·PF₆ were also studied by LSIMS, where complex formation was evidenced by the discovery of strong peaks corresponding to the 1:1 complexes with the loss of their PF₆[−] counterions.^[22]

Table 1. ¹H NMR spectroscopic data^[a] (δ values) for 1) DB24C8,^[b] 2) the carboxyl-substituted dibenzylammonium salts **2**·PF₆–**6**·PF₆,^[b] and 3) the associated [2]pseudorotaxanes in CD₃CN at 20 °C.^[c]

	Crown ether		Dibenzylammonium cation		
	OCH ₂	(RO) ₂ ArH	CH ₂ NH ₂ ⁺	PhH	(HO ₂ C) _n ArH
DB24C8	3.67 (s, 8H), 3.79 (m, 8H), 4.08 (m, 8H)	6.85–6.96 (m, 8H)	–	–	–
2 ·PF ₆	–	–	4.25 (s, 2H), 4.29 (s, 2H)	7.46 (s, 5H)	7.57 (d, 2H), 8.06 (d, 2H)
[DB24C8· 2][PF ₆]	3.49–3.63 (m, 8H), 3.74 (m, 8H), 3.95–4.06 (m, 8H)	6.71–6.84 (m, 8H)	4.66 (m, 2H), 4.79 (m, 2H)	7.22–7.30 (m, 5H)	7.38 (d, 2H), 7.65 (d, 2H)
3 ·PF ₆	–	–	4.25 (s, 2H), 4.31 (s, 2H)	7.46 (s, 5H)	7.58 (t, 1H), 7.71 (d, 1H), 8.07 (d, 1H), 8.16 (s, 1H)
[DB24C8· 3][PF ₆]	3.51–3.65 (m, 8H), 3.77 (m, 8H), 3.94–4.06 (m, 8H)	6.70–6.83 (m, 8H)	4.64 (m, 2H), 4.81 (m, 2H)	7.25–7.34 (m, 5H)	7.12 (t, 1H), 7.42 (d, 1H), 7.62 (d, 1H), 8.00 (s, 1H)
4 ·PF ₆	–	–	4.31 (s, 4H)	–	7.56 (d, 4H), 8.06 (d, 4H)
[DB24C8· 4][PF ₆]	3.58 (s, 8H), 3.77 (m, 8H), 4.01 (m, 8H)	6.70–6.81 (m, 8H)	4.78 (m, 4H)	–	7.44 (d, 4H), 7.75 (d, 4H)
5 ·PF ₆	–	–	4.31 (s, 4H)	–	7.59 (t, 2H), 7.69 (d, 2H), 8.07 (d, 2H), 8.13 (s, 2H)
[DB24C8· 5][PF ₆]	3.62 (s, 8H), 3.78 (m, 8H), 4.00 (m, 8H)	6.67–6.81 (m, 8H)	4.75 (m, 4H)	–	7.26 (t, 2H), 7.54 (d, 2H), 7.76 (d, 2H), 8.06 (s, 2H)
6 ·PF ₆	–	–	4.25 (s, 2H), 4.38 (s, 2H)	7.46 (s, 5H)	8.35 (s, 2H), 8.58 (s, 1H)
[DB24C8· 6][PF ₆]	^[d]	6.55–6.73 (m, 8H)	4.61 (m, 2H), 4.94 (m, 2H)	7.38–7.55 (m, 5H)	7.85 (s, 1H), 8.09 (s, 2H)

[a] The ¹H NMR spectra were recorded on a Bruker AC300 spectrometer (at 300.1 MHz) with CD₃CN solvent as the lock and the multiplet observed for the residual protons of this solvent (at $\delta = 1.93$) as internal reference. [b] The concentration of both components was 1.0×10^{-2} M. [c] Signals were observed simultaneously for both the uncomplexed crown ether and salt, in addition to the [2]pseudorotaxane complex. [d] A complicated band of signals was observed from $\delta = 3.55$ – 4.15 in the ¹H NMR spectrum of a 1:1 mixture of DB24C8 and **6**·PF₆, so that it was not possible to correlate signals associated with the OCH₂ protons to the uncomplexed or complexed DB24C8 macrocycle.

Table 2. Association constants (K_a) and related free energies of complexation ($-\Delta G^\circ$) for the [2]pseudorotaxane complexes formed between DB24C8 and the dibenzylammonium salts **1**·PF₆–**6**·PF₆ in CD₃CN at 20 °C.

	K_a (M ^{−1}) ^[a]	$-\Delta G^\circ$ (kcal mol ^{−1}) ^[b]
[DB24C8· 1][PF ₆]	420	3.6
[DB24C8· 2][PF ₆]	610	3.7
[DB24C8· 3][PF ₆]	480	3.6
[DB24C8· 4][PF ₆]	950	4.0
[DB24C8· 5][PF ₆]	880	3.9
[DB24C8· 6][PF ₆]	1500	4.3

[a] Association constants (K_a) were obtained by means of single-point measurements of the concentrations of the complexed and uncomplexed species, from the relevant ¹H NMR spectra at 20 °C, by the relationship $K_a = [\text{DB24C8} \cdot \text{salt}]/[\text{DB24C8}][\text{salt}]$ (percentage error $\leq 15\%$). [b] The free energies of complexation ($-\Delta G^\circ$) were calculated from the K_a values with the expression $-\Delta G^\circ = RT \ln K_a$.

Complex formation was indicated (Table 3) from the ¹H NMR spectra of 1:2 mixtures of BPP34C10 with the ammonium salts **2**·PF₆–**6**·PF₆, where substantial chemical shift changes were detected for the signals^[23] observed for both the host and the guest in CD₂Cl₂/CD₃CN (2:1). However, in this mixed solvent system, all of the resonances were sharp and well-defined, indicating that the medium is too polar for interpseudorotaxane association to occur through the carboxyl groups.^[24] LSIMS provided proof of the existence of the 1:2

pseudorotaxane complexes in the gas phase. The LSIMS, obtained from 1:2 molar solutions of BPP34C10 with the salts $2 \cdot \text{PF}_6^- - 6 \cdot \text{PF}_6^-$, displayed peaks for the 1:2 complexes (with the loss of one PF_6^- counterion) in all cases. However, these peaks were extremely small compared with the base peaks in the spectra, indicating that, as noted previously,^[7c] it is extremely difficult to characterize three-component pseudorotaxane supermolecules, such as these, in the gas phase.

X-ray crystallography (supramolecular synthesis): The X-ray crystallographic analysis of the 1:1 complex formed between DB24C8 and the 2^+ cation shows (Figure 4A) the DB24C8 macrocycle to adopt a V-shaped conformation, with the cation threaded through the center of the macroring to form a [2]pseudorotaxane. Complex stabilization is achieved by means of a combination of $\text{N}^+ - \text{H} \cdots \text{O}$ and $\text{C} - \text{H} \cdots \text{O}$ hydrogen bonds and a face-to-face aryl–aryl stacking interaction between the π -electron-deficient benzoic acid ring of the ammonium cation and one of the π -electron-rich catechol rings of the DB24C8 macrocycle (the mean interplanar separation is 3.71 Å, with a centroid–centroid distance of 4.12 Å, the rings being inclined by ca. 15°). Even though there is an approach of 4.18 Å between the centroids of the other catechol unit of the crown ether and the benzoic acid ring, the rings are inclined by ca. 29°, thereby precluding any significant $\pi - \pi$ stacking interaction. Inspection of the packing of this pseudorotaxane shows glide-related complexes to be linked in

a head-to-tail fashion (via bifurcated hydrogen bonds between the carboxyl hydrogen atom of one pseudorotaxane unit and the oxygen atoms of a catechol ring of the next) to generate an interwoven supramolecular architecture that is reminiscent of a *daisy chain* (Figure 4B,C).^[25] This polymeric supramolecular architecture presumably originates as a result of the $\pi - \pi$ stacking interaction, in addition to the V-shaped conformation of the polyether. The combination of these two factors means that the head-on dimerization of the [DB24C8 · 2]⁺ pseudorotaxane, using the carboxyl dimer supramolecular synthon, is disfavored, since the catechol units from adjacent pseudorotaxanes would be in very close proximity to one another, resulting in detrimental nonbonding interactions.

The X-ray analysis of the 1:1 complex formed between the DB24C8 macrocycle and the cation 4^+ reveals that, in this instance, the interpenetrated DB24C8 macroring has an extended approximately C_1 -symmetric conformation with its phenoxyethylene units roughly coplanar with their associated catechol rings, a conformation very similar to that adopted by the uncomplexed DB24C8 macrocycle.^[26] As a result of a combination of $\text{N}^+ - \text{H} \cdots \text{O}$ and $\text{C} - \text{H} \cdots \text{O}$ hydrogen-bonding interactions (Figure 5A), the cation is threaded asymmetrically through the center of the polyether macroring and has one of its benzoic acid rings oriented approximately parallel to, and overlying, one of the catechol rings of the DB24C8 macrocycle (the mean interplanar separation is 3.74 Å with a centroid–centroid distance of 3.91 Å, the rings being inclined

Table 3. ¹H NMR spectroscopic data^[a] (δ values) for 1) BPP34C10,^[b] 2) the carboxyl-substituted dibenzylammonium salts $2 \cdot \text{PF}_6^- - 6 \cdot \text{PF}_6^-$,^[b] and 3) 1:2 mixtures^[b,c] of the two compounds in $\text{CD}_2\text{Cl}_2/\text{CD}_3\text{CN}$ (2:1) at 20 °C.

	Crown ether		Dibenzylammonium cation		
	OCH_2	$(\text{RO})_2\text{ArH}$	CH_2NH_2^+	PhH	$(\text{HO}_2\text{C})_n\text{ArH}$
BPP34C10	3.58 (m, 16H), 3.71 (m, 8H), 3.92 (m, 8H)	6.69 (s, 8H)	–	–	–
$2 \cdot \text{PF}_6^-$	–	–	4.18 (s, 4H), 4.22 (s, 4H)	7.43 (s, 10H)	7.49 (d, 4H), 8.04 (d, 4H)
BPP34C10 + $2 \cdot \text{PF}_6^-$	3.45–3.59 (m, 16H), 3.71 (m, 8H), 3.95 (m, 8H)	6.69 (s, 8H)	4.12 (s, 4H), 4.14 (s, 4H)	7.38–7.49 (m, 10H)	7.34 (d, 4H), 7.94 (d, 4H)
$3 \cdot \text{PF}_6^-$	–	–	4.16 (s, 4H), 4.21 (s, 4H)	7.40 (s, 10H)	7.51 (t, 2H), 7.62 (d, 2H), 8.04 (d, 2H), 8.10 (s, 2H)
BPP34C10 + $3 \cdot \text{PF}_6^-$	3.54 (s, 16H), 3.69 (m, 8H), 3.86 (m, 8H)	6.60 (s, 8H)	4.15 (s, 8H)	7.42 (s, 10H)	7.47 (d, 2H), 7.53 (t, 2H), 7.81 (s, 2H), 7.99 (d, 2H)
$4 \cdot \text{PF}_6^-$	–	–	4.21 (s, 8H)	–	7.49 (d, 8H), 8.03 (d, 8H)
BPP34C10 + $4 \cdot \text{PF}_6^-$	3.48–3.59 (m, 16H), 3.70 (m, 8H), 3.91 (m, 8H)	6.65 (s, 8H)	4.19 (br, 8H)	–	7.40 (d, 8H), 7.96 (d, 8H)
$5 \cdot \text{PF}_6^-$	–	–	4.22 (s, 8H)	–	7.50 (t, 4H), 7.61 (d, 4H), 8.00 (d, 4H), 8.07 (s, 4H)
BPP34C10 + $5 \cdot \text{PF}_6^-$	3.55 (s, 16H), 3.70 (m, 8H), 3.89 (m, 8H)	6.63 (s, 8H)	4.18 (s, 8H)	–	7.48–7.54 (m, 8H), 7.85 (s, 4H), 7.93 (d, 4H)
$6 \cdot \text{PF}_6^-$	–	–	4.18 (s, 4H), 4.28 (s, 4H)	7.40 (s, 10H)	8.30 (s, 4H), 8.59 (s, 2H)
BPP34C10 + $6 \cdot \text{PF}_6^-$	3.55 (s, 16H), 3.69 (m, 8H), 3.87 (m, 8H)	6.58 (s, 8H)	4.18 (br, 8H)	7.43 (s, 10H)	8.10 (s, 4H), 8.50 (s, 2H)

[a] The ¹H NMR spectra were recorded on a Bruker AC300 spectrometer (at 300.1 MHz) with CD_3CN solvent as the lock and the residual solvent peak as internal reference. [b] The concentration of BPP34C10 was 4.2×10^{-3} M, while that of the salts was 8.4×10^{-3} M. [c] In contrast to the spectra described in Table 1, time-averaged sets of signals are observed for both host and guest species in the ¹H NMR spectra, since fast kinetic exchange is occurring between uncomplexed and complexed states on the ¹H NMR time scale.

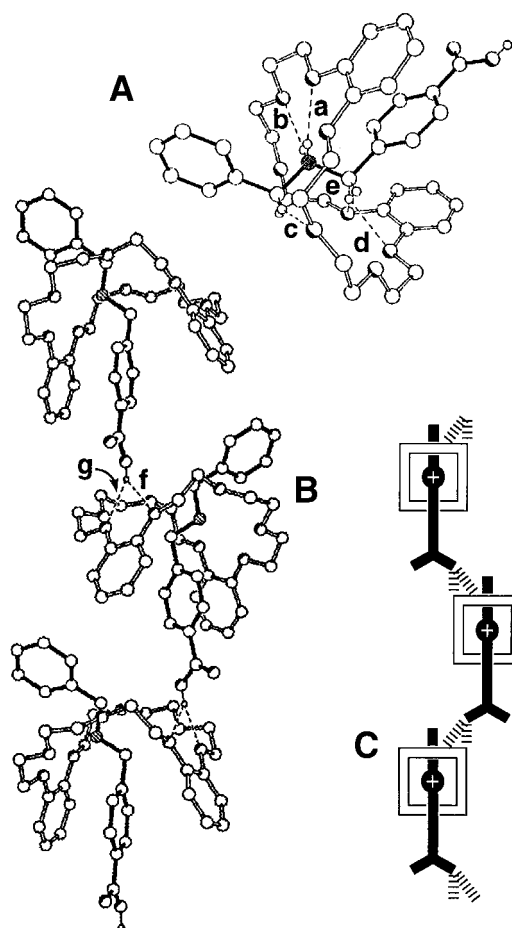


Figure 4. A: Crystal structure of the $[\text{DB24C8}\cdot 2]^+$ pseudorotaxane. Bond lengths and angles for hydrogen bonds: a) $\text{N}^+\cdots\text{O}$ 2.92 Å, $\text{H}\cdots\text{O}$ 2.15 Å, $\text{N}^+-\text{H}\cdots\text{O}$ 142°; b) $\text{N}^+\cdots\text{O}$ 2.90 Å, $\text{H}\cdots\text{O}$ 2.13 Å, $\text{N}^+-\text{H}\cdots\text{O}$ 144°; c) $\text{C}\cdots\text{O}$ 3.18 Å, $\text{H}\cdots\text{O}$ 2.26 Å, $\text{C}-\text{H}\cdots\text{O}$ 159°; d) $\text{C}\cdots\text{O}$ 3.25 Å, $\text{H}\cdots\text{O}$ 2.46 Å, $\text{C}-\text{H}\cdots\text{O}$ 139°; e) $\text{C}\cdots\text{O}$ 3.36 Å, $\text{H}\cdots\text{O}$ 2.50 Å, $\text{C}-\text{H}\cdots\text{O}$ 148°. B: The hydrogen-bonded supramolecular array—resembling a daisy chain—produced by the noncovalent polymerization of the $[\text{DB24C8}\cdot 2]^+$ pseudorotaxane in the solid state. Bond lengths and angles for hydrogen bonds: f) $\text{O}\cdots\text{O}$ 3.06 Å, $\text{H}\cdots\text{O}$ 2.25 Å, $\text{O}-\text{H}\cdots\text{O}$ 150°; g) $\text{O}\cdots\text{O}$ 2.92 Å, $\text{H}\cdots\text{O}$ 2.20 Å, $\text{O}-\text{H}\cdots\text{O}$ 136°. C: Cartoon representation of the daisy-chain-like supramolecular array $[\text{DB24C8}\cdot 2]^+_n$.

by ca. 13°). The other benzoic acid ring of the cation is oriented approximately axially with respect to the DB24C8 macroring. An examination of interpseudorotaxane association (Figure 5B,C) reveals that two $[\text{DB24C8}\cdot 4]^+$ complexes stack, via the benzoic acid ring that is excluded from intrapseudorotaxane $\pi-\pi$ stacking (the centroid–centroid and interplanar separations are 4.19 and 3.79 Å, respectively), to generate a dimer of C_1 -related [2]pseudorotaxanes. This pseudorotaxane dimer is further stabilized by pairs of $\text{O}-\text{H}\cdots\text{O}$ hydrogen bonds between one of the carboxyl moieties of the 4⁺ cation and an oxygen atom in one of the polyether linkages of the DB24C8 macrocycle of a symmetry-related [2]pseudorotaxane and vice versa. Further propagation of this recognition motif is halted by the intervention of an Me_2CO solvent molecule, which is hydrogen-bonded to the vacant carboxyl donor site attached to the aryl ring that is involved in intrapseudorotaxane $\pi-\pi$ stacking. This crystal structure convincingly demonstrates a fundamental difficulty associated with crystal engineering. Here, the anticipated carboxylic

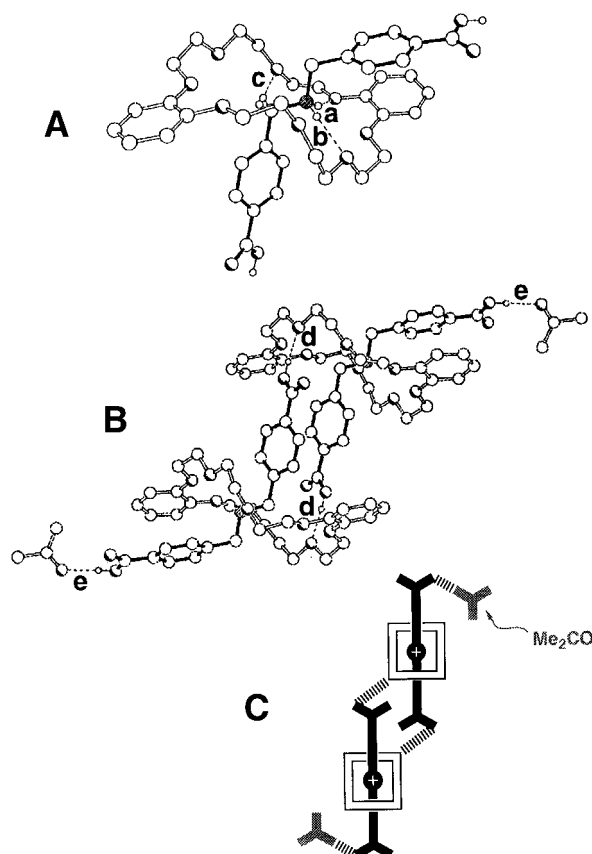


Figure 5. A: View of the structure of the $[\text{DB24C8}\cdot 4]^+$ pseudorotaxane in the solid state. Bond lengths and angles for hydrogen bonds: a) $\text{N}^+\cdots\text{O}$ 3.11 Å, $\text{H}\cdots\text{O}$ 2.26 Å, $\text{N}^+-\text{H}\cdots\text{O}$ 158°; b) $\text{N}^+\cdots\text{O}$ 3.02 Å, $\text{H}\cdots\text{O}$ 2.14 Å, $\text{N}^+-\text{H}\cdots\text{O}$ 165°; c) $\text{C}\cdots\text{O}$ 3.21 Å, $\text{H}\cdots\text{O}$ 2.37 Å, $\text{C}-\text{H}\cdots\text{O}$ 145°. B: Association of two Me_2CO molecules with each of the pendant carboxyl groups of the $\{[\text{DB24C8}\cdot 4]^+\}_2$ species formed by aryl–aryl stacking and hydrogen-bonding interactions. Bond lengths and angles for hydrogen bonds: d) $\text{O}\cdots\text{O}$ 2.73 Å, $\text{H}\cdots\text{O}$ 1.85 Å, $\text{O}-\text{H}\cdots\text{O}$ 165°; e) $\text{O}\cdots\text{O}$ 2.78 Å, $\text{H}\cdots\text{O}$ 1.88 Å, $\text{O}-\text{H}\cdots\text{O}$ 173°. C: Cartoon representation depicting the $\{[\text{DB24C8}\cdot 4]^+\}_2\cdot 2\text{Me}_2\text{CO}$ species.

acid dimer pairs are not observed, presumably because interpseudorotaxane $\pi-\pi$ stacking interactions act as the dominant factor that determines the packing of the $[\text{DB24C8}\cdot 4]^+$ species.

The coconformation^[27] of the $[\text{DB24C8}\cdot 5]^+$ [2]pseudorotaxane (Figure 6A) is remarkably similar to that of its congener $[\text{DB24C8}\cdot 4]^+$. Nevertheless, although there are small amounts of Me_2CO solvent in the crystals of the $[\text{DB24C8}\cdot 5]^+$ complex, it does not interfere with the expected hydrogen-bonding pattern: supramolecular polymerization, employing the carboxyl dimer supramolecular synthon, leads to the *main-chain, hydrogen-bonded pseudopolyrotaxane*^[15] superstructure illustrated in Figure 6B,C.

The X-ray analysis of the 1:1 complex formed between DB24C8 and **6**· PF_6 (Figure 7A) reveals a very similar coconformation,^[27] for the threading of the cation through the center of the DB24C8 crown ether macroring, to that observed for the related complex $[\text{DB24C8}\cdot 2]^+$. The cation has a typical all-*anti* geometry for its $\text{C}-\text{CH}_2-\text{NH}_2^+-\text{CH}_2-\text{C}$ backbone, but the differences in orientations of the isophthalate and benzyl rings result in a marked departure from the normal gull-wing conformation: the isophthalate ring is

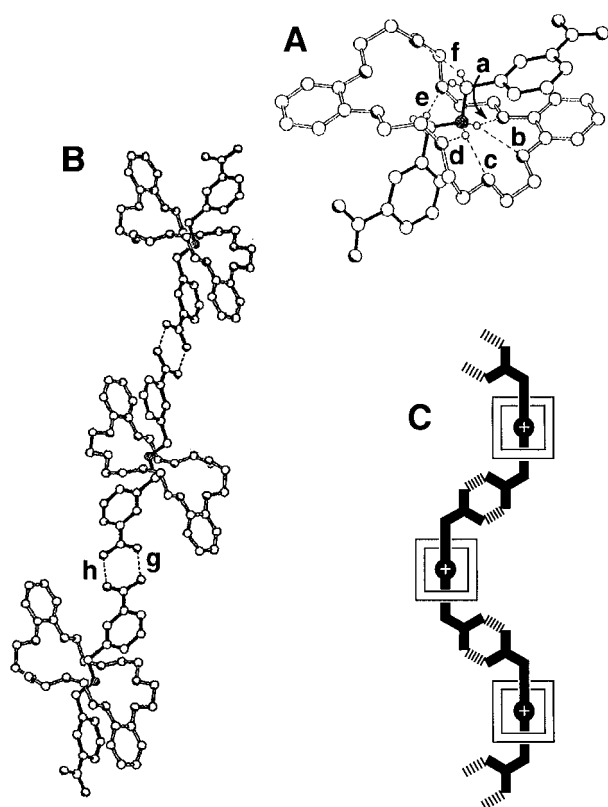


Figure 6. A: The crystal structure of the $[\text{DB24C8}\cdot\mathbf{5}]^+$ pseudorotaxane. Hydrogen bonding distances and angles: a) $\text{N}^+\cdots\text{O}$ 3.12 Å, $\text{H}\cdots\text{O}$ 2.28 Å, $\text{N}^+-\text{H}\cdots\text{O}$ 157°; b) $\text{N}^+\cdots\text{O}$ 3.01 Å, $\text{H}\cdots\text{O}$ 2.32 Å, $\text{N}^+-\text{H}\cdots\text{O}$ 133°; c) $\text{N}^+\cdots\text{O}$ 3.02 Å, $\text{H}\cdots\text{O}$ 2.20 Å, $\text{N}^+-\text{H}\cdots\text{O}$ 151°; d) $\text{N}^+\cdots\text{O}$ 3.05 Å, $\text{H}\cdots\text{O}$ 2.34 Å, $\text{N}^+-\text{H}\cdots\text{O}$ 136°; e) $\text{C}\cdots\text{O}$ 3.16 Å, $\text{H}\cdots\text{O}$ 2.52 Å, $\text{C}-\text{H}\cdots\text{O}$ 157°; f) $\text{C}\cdots\text{O}$ 3.32 Å, $\text{H}\cdots\text{O}$ 2.49 Å, $\text{C}-\text{H}\cdots\text{O}$ 145°. B: The main-chain, hydrogen-bonded pseudopolyrotaxane produced by the noncovalent polymerization of the $[\text{DB24C8}\cdot\mathbf{5}]^+$ pseudorotaxane by means of the carboxyl dimer supramolecular synthon. Hydrogen bond lengths: g) $\text{O}\cdots\text{O}$ 2.63 Å; h) $\text{O}\cdots\text{O}$ 2.63 Å. C: Cartoon of the $\{[\text{DB24C8}\cdot\mathbf{5}]^+\}_n$ pseudopolyrotaxane.

inclined by 81° to the plane of the backbone, while the benzyl ring is inclined by only 23°. Complex stabilization is again achieved by a combination of $\text{N}^+-\text{H}\cdots\text{O}$ and $\text{C}-\text{H}\cdots\text{O}$ hydrogen bonds along with a $\pi-\pi$ stacking interaction between the isophthalate ring and one of the catechol rings of the DB24C8 macrocycle (the associated centroid–centroid and mean interplanar separations are 3.79 and 3.48 Å, respectively). As observed for the $[\text{DB24C8}\cdot\mathbf{2}]^+$ superstructure, there is a relatively short contact (4.12 Å) between the center of the isophthalic acid ring and the other catechol ring of the DB24C8 macrocycle. However, these rings are inclined by 26°, thus precluding any significant $\pi-\pi$ interaction. The packing of the $[\text{DB24C8}\cdot\mathbf{6}]^+$ complexes (Figure 7B,C) reveals the formation of a *side-chain, hydrogen-bonded pseudopolyrotaxane*^[15,28] superstructure, with one of the carboxylic acid units of one cation linking to the other of the next through the carboxyl dimer. Presumably, the formation of this supramolecular polymer is allowed, in this instance, since the catechol units of the pseudorotaxane monomers approach each other in a sterically less demanding side-on fashion as opposed to a head-on fashion (see $[\text{DB24C8}\cdot\mathbf{2}]^+$). Inspection of the packing of the pseudopolyrotaxane chains does not reveal any significant interchain interactions.

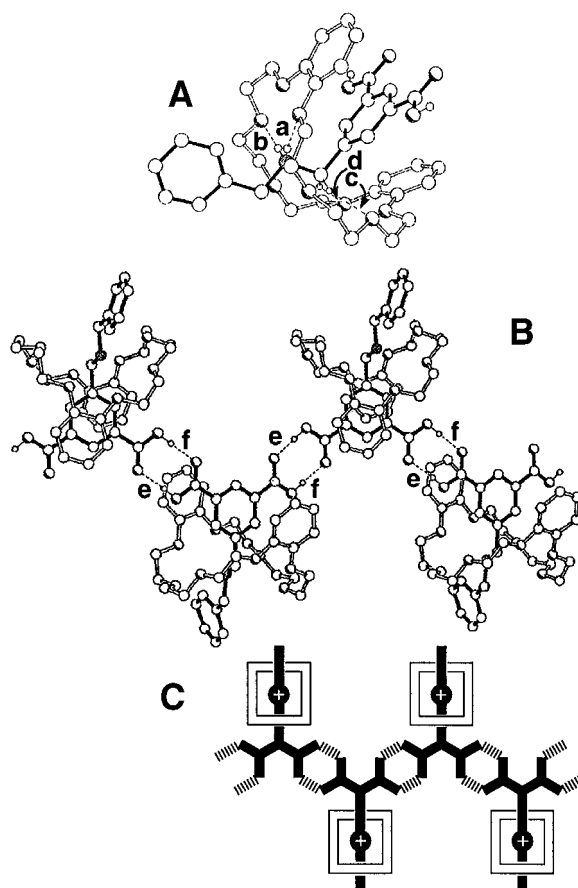


Figure 7. A: The structure of the $[\text{DB24C8}\cdot\mathbf{6}]^+$ pseudorotaxane in the solid state. Bond lengths and angles for hydrogen bonds: a) $\text{N}^+\cdots\text{O}$ 3.04 Å, $\text{H}\cdots\text{O}$ 2.15 Å, $\text{N}^+-\text{H}\cdots\text{O}$ 170°; b) $\text{N}^+\cdots\text{O}$ 2.88 Å, $\text{H}\cdots\text{O}$ 1.98 Å, $\text{N}^+-\text{H}\cdots\text{O}$ 179°; c) $\text{C}\cdots\text{O}$ 3.30 Å, $\text{H}\cdots\text{O}$ 2.39 Å, $\text{C}-\text{H}\cdots\text{O}$ 156°; d) $\text{C}\cdots\text{O}$ 3.27 Å, $\text{H}\cdots\text{O}$ 2.40 Å, $\text{C}-\text{H}\cdots\text{O}$ 150°. B: The side-chain, hydrogen-bonded pseudopolyrotaxane produced by the noncovalent polymerization of the $[\text{DB24C8}\cdot\mathbf{6}]^+$ pseudorotaxane by means of the carboxyl dimer supramolecular synthon. Bond lengths and angles for hydrogen bonds: e) $\text{O}\cdots\text{O}$ 2.60 Å, $\text{H}\cdots\text{O}$ 1.73 Å, $\text{O}-\text{H}\cdots\text{O}$ 163°; f) $\text{O}\cdots\text{O}$ 2.64 Å, $\text{H}\cdots\text{O}$ 1.75 Å, $\text{O}-\text{H}\cdots\text{O}$ 176°. C: Cartoon representation of the side-chain, hydrogen-bonded pseudopolyrotaxane $\{[\text{DB24C8}\cdot\mathbf{6}]^+\}_n$.

The X-ray crystallographic analysis of the 1:2 complex formed between the BPP34C10 macrocycle and the cation $\mathbf{2}^+$ (Figure 8) reveals^[17] that both of the cations are threaded codirectionally through the center of the macrocycle to produce a [3]pseudorotaxane that is stabilized by five $\text{N}^+-\text{H}\cdots\text{O}$ hydrogen bonds between the NH_2^+ centers and oxygen atoms from each of the polyether loops in the macrocycle. Secondary stabilization of the [3]pseudorotaxane superarchitecture is achieved by an edge-to-face $\text{C}-\text{H}\cdots\pi$ contact between one of the methylene hydrogen atoms of the 4-carboxybenzyl group and one of the hydroquinone rings of the BPP34C10 macrocycle (the associated $\text{H}\cdots\pi$ distance and $\text{C}-\text{H}\cdots\pi$ angle are 2.88 Å and 143°, respectively). The centroid–centroid separation between the benzoic acid rings of independent $\mathbf{2}^+$ cations is ca. 4.6 Å, the rings being tilted by 28°, thereby excluding any meaningful aryl–aryl stacking interactions. An additional feature of the superstructure, which is of particular interest, is the directing of a fluorine atom from one of the PF_6^- anions into the cleft between the two dialkylammonium cations; it lies at a distance of ca. 2.5 Å

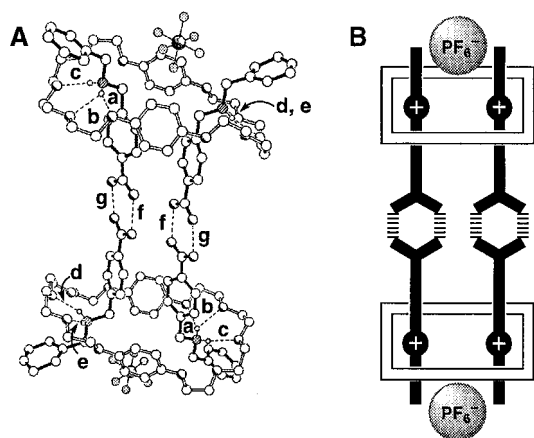


Figure 8. A: View of the $[[\text{BPP34C10} \cdot (\text{2})_2]^{2+}]_2$ supermolecule (produced by the noncovalent dimerization of the $[\text{BPP34C10} \cdot (\text{2})_2]^{2+}$ pseudorotaxane by means of the carboxyl dimer supramolecular synthon) in the solid state, showing the PF_6^- anions that may assist the self-assembly of the supermolecule. Bond lengths and angles for hydrogen bonds: a) $\text{N}^+ \cdots \text{O}$ 3.18 Å, $\text{H} \cdots \text{O}$ 2.33 Å, $\text{N}^+ - \text{H} \cdots \text{O}$ 157°; b) $\text{N}^+ \cdots \text{O}$ 2.98 Å, $\text{H} \cdots \text{O}$ 2.32 Å, $\text{N}^+ - \text{H} \cdots \text{O}$ 130°; c) $\text{N}^+ \cdots \text{O}$ 2.93 Å, $\text{H} \cdots \text{O}$ 2.06 Å, $\text{N}^+ - \text{H} \cdots \text{O}$ 161°; d) $\text{N}^+ \cdots \text{O}$ 2.86 Å, $\text{H} \cdots \text{O}$ 2.19 Å, $\text{N}^+ - \text{H} \cdots \text{O}$ 130°; e) $\text{N}^+ \cdots \text{O}$ 2.93 Å, $\text{H} \cdots \text{O}$ 2.06 Å, $\text{N}^+ - \text{H} \cdots \text{O}$ 163°; f) $\text{O} \cdots \text{O}$ 2.68 Å; g) $\text{O} \cdots \text{O}$ 2.61 Å. B: Cartoon portraying the $[[\text{BPP34C10} \cdot (\text{2})_2]^{2+}]_2 \cdot 2\text{PF}_6^-$ species.

from the benzylic hydrogen atoms of one of the cations.^[29] A similar approach of ca. 2.5 Å is also evident between one of the equatorial fluorine atoms of this anion and one of the hydrogen atoms of a hydroquinone ring. We hypothesize that this PF_6^- anion may assist^[7f] the macrocyclic polyether by helping to align the two carboxyl groups of the [3]pseudorotaxane codirectionally with respect to each other, leading to the noncovalent dimerization of pairs of C_i symmetrically-related [3]pseudorotaxanes to generate doubly-encircled six-component organic supermolecules that are linked through pairs of strong $\text{O}-\text{H} \cdots \text{O}$ hydrogen bonds (Figure 8), both involving carboxyl dimers. In many respects, the structure of this six-component assemblage is similar to that of the 2:2 complex formed between α, α' -bis(benzylammonium)-*p*-xylylene bis(hexafluorophosphate) and BPP34C10,^[7b-c] an observation that is hardly surprising, given the fact that the carboxyl dimer may be regarded as a surrogate for a *p*-disubstituted benzene ring.^[11b]

The analogous 1:2 complex formed between BPP34C10 and 3^+ , in which the carboxyl substituent is located in the *meta* position, possesses a very similar supramolecular architecture to that of the $[\text{BPP34C10} \cdot (\text{2})_2]^{2+}$ complex. Pairs of cations thread codirectionally through the BPP34C10 macrocycle and are hydrogen bonded, through the carboxyl groups, to their immediate neighbors in C_i -related 1:2 complexes (Figure 9). In essence, the only significant change in the overall superstructure is a shearing of one of the BPP34C10 rings in one $[\text{BPP34C10} \cdot (\text{3})_2]^{2+}$ pseudorotaxane with respect to that of its hydrogen-bonded counterpart. Once again, complex stabilization is achieved by means of the same $\text{N}^+ - \text{H} \cdots \text{O}$ and $\text{O} - \text{H} \cdots \text{O}$ hydrogen bonds that were observed in the $[[\text{BPP34C10} \cdot (\text{2})_2]^{2+}]_2$ superstructure. Although there is a near-parallel alignment of the pairs of benzoic acid rings (the mean interplanar separation is ca. 3.62 Å), they are offset (the centroid-centroid separation is 4.99 Å) such as to

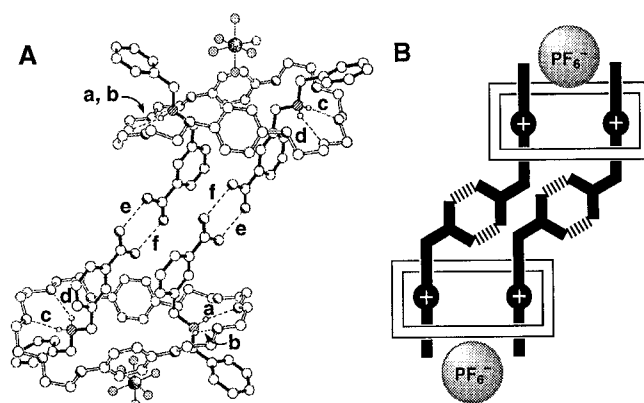


Figure 9. A: View of the crystal structure of the $[[\text{BPP34C10} \cdot (\text{3})_2]^{2+}]_2$ supermolecule produced by the noncovalent dimerization of the $[\text{BPP34C10} \cdot (\text{3})_2]^{2+}$ pseudorotaxane by means of the carboxyl dimer supramolecular synthon, showing the PF_6^- anions located in the clefts between two neighboring 3^+ cations. Bond lengths and angles for hydrogen bonds: a) $\text{N}^+ \cdots \text{O}$ 2.92 Å, $\text{H} \cdots \text{O}$ 2.11 Å, $\text{N}^+ - \text{H} \cdots \text{O}$ 149°; b) $\text{N}^+ \cdots \text{O}$ 2.90 Å, $\text{H} \cdots \text{O}$ 2.13 Å, $\text{N}^+ - \text{H} \cdots \text{O}$ 142°; c) $\text{N}^+ \cdots \text{O}$ 2.90 Å, $\text{H} \cdots \text{O}$ 2.07 Å, $\text{N}^+ - \text{H} \cdots \text{O}$ 153°; d) $\text{N}^+ \cdots \text{O}$ 2.92 Å, $\text{H} \cdots \text{O}$ 2.18 Å, $\text{N}^+ - \text{H} \cdots \text{O}$ 139°; e) $\text{O} \cdots \text{O}$ 2.57 Å; f) $\text{O} \cdots \text{O}$ 2.67 Å. B: Cartoon depicting the $[[\text{BPP34C10} \cdot (\text{3})_2]^{2+}]_2 \cdot 2\text{PF}_6^-$ supermolecule.

preclude any significant $\pi-\pi$ stacking between them. A particularly interesting feature of this six-component assemblage is the positioning (Figure 9) of one of the PF_6^- anions within the cleft formed between the two 3^+ cations, an arrangement that is almost identical to that observed for the $[\text{BPP34C10} \cdot (\text{2})_2]^{2+}$ complex. In the crystal lattice, this anion is notable for its order and for the proximal relationship between its fluorine atoms and pairs of hydroquinone hydrogen atoms on the BPP34C10 macrocyclic ring (there are three $\text{H} \cdots \text{F}$ distances of less than 2.5 Å). We feel that this recurrence of a selective positioning of one of these anions reinforces our conclusion (vide supra) that this anion may be assisting^[7f] the polyether in enforcing the codirectionality of the benzoic acid rings, thus allowing the production of the discrete multi-component assemblage.

Contrasting with the crystal structures of the $[\text{BPP34C10} \cdot (\text{2})_2]^{2+}$ and $[\text{BPP34C10} \cdot (\text{3})_2]^{2+}$ pseudorotaxanes, the X-ray crystallographic analysis^[17] of the 1:2 complex formed between the BPP34C10 macrocycle and the isophthalic acid-substituted cation 6^+ (Figure 10A) reveals that the secondary dialkylammonium strands are, in this instance, threaded centrosymmetrically with respect to one another—that is, in an *antiparallel* fashion—presumably since, in this case, no PF_6^- anions are involved in the self-assembly process (vide infra). Once again, stabilization of the [3]pseudorotaxane superstructure is achieved by $\text{N}^+ - \text{H} \cdots \text{O}$ hydrogen bonds between the NH_2^+ centers and pairs of oxygen atoms in each of the polyether arcs of the macrocycle. The cations maintain the normal gull-wing conformation, with a planar all-*anti* $\text{C}-\text{CH}_2-\text{NH}_2^+-\text{CH}_2-\text{C}$ backbone, though with the isophthalate ring markedly skewed from an orthogonal relationship. Noncovalent association occurs between the pairs of carboxyl groups of each cation and their nonequivalent counterparts in symmetry-related complexes as a result of strong $\text{O}-\text{H} \cdots \text{O}$ hydrogen bonding between the carboxyl groups. In this case, the outcome of combining multiple carboxyl dimer and

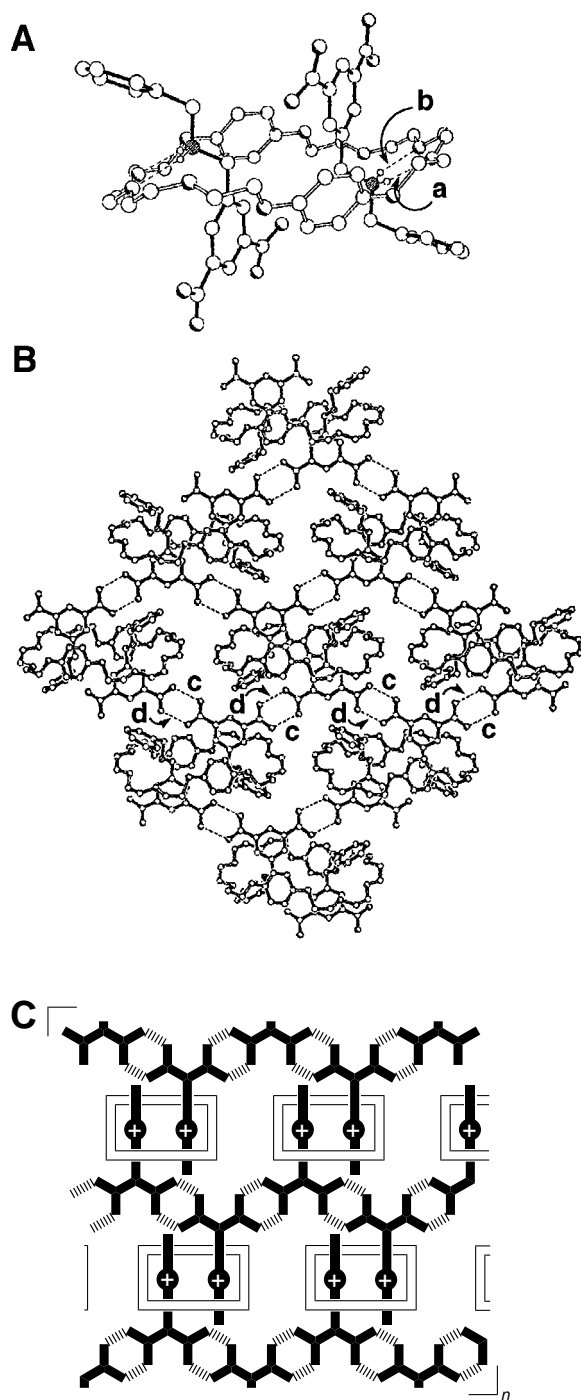


Figure 10. A: The crystal structure of the [BPP34C10·(6)₂]²⁺ pseudorotaxane. Bond lengths and angles for hydrogen bonds: a) N⁺...O 2.88 Å, H...O 2.09 Å, N⁺–H...O 145°; b) N⁺...O 2.87 Å, H...O 2.09 Å, N⁺–H...O 146°. B: The interwoven supramolecular cross-linked polymer formed through the noncovalent polymerization of the [BPP34C10·(6)₂]²⁺ pseudorotaxane by means of the carboxyl dimer supramolecular synthon. Hydrogen bond lengths: c) O...O 2.57 Å; d) O...O 2.69 Å. C: Cartoon illustrating the interwoven supramolecular cross-linked polymer {[BPP34C10·(6)₂]²⁺}_n.

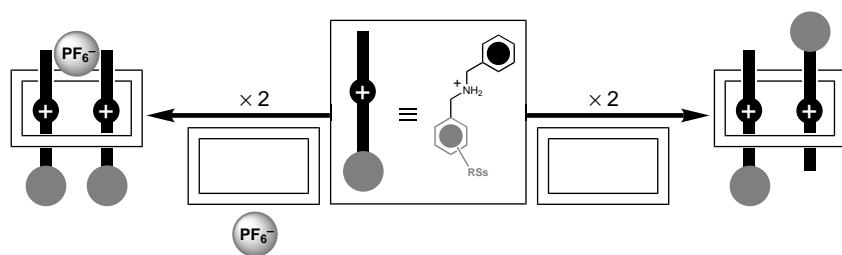
double threading motifs is the production of a novel type of supramolecular polymer (Figure 10B,C),^[30] specifically, an *interwoven supramolecular cross-linked polymer*, in which cross-linking of isophthalic acid tapes^[13] (cf. Figure 2B) is induced by the macrocyclic polyether, since it guides two

isophthalic acid units from separate 6⁺ cations in opposing directions, that is, the tapes are interlinked through the [3]pseudorotaxane unit to form two-dimensional pseudopolyrotaxane^[15] sheets. The sheets are fairly thick (ca. 12.5 Å) since the planes of the O–H...O hydrogen bonds are approximately orthogonal to the planes of the BPP34C10 macrocycle. Included PhH solvent molecules and disordered PF₆[−] counterions are located in the interstices between the polymeric layers. Neither of these species play significant roles in establishing the pseudopolyrotaxane sheet superstructure.

The crystal structures of the [3]pseudorotaxanes described above demonstrate^[17] that the ditopic crown ether BPP34C10 acts as a useful unit for solid-state supramolecular synthesis in that it can, to a certain extent, direct supramolecular recognition sites in space (Scheme 2), leading to the creation of multiply encircled supermolecules and interwoven supramolecular arrays, that is, the crown ether induces *supramolecular preorganization* of the benzoic or isophthalic acid subunits for further noncovalent association using the carboxyl dimer supramolecular synthon. In fact, superstructures comparable to the {[BPP34C10·(2)₂]²⁺}₂, {[BPP34C10·(3)₂]²⁺}₂, and {[BPP34C10·(6)₂]²⁺}_n architectures have been observed in the crystal structures of species in which *molecular preorganization*^[31] dictates the spatial disposition of benzoate or isophthalate moieties by covalent frameworks. *Molecular* bis-carboxylic acids that are endowed with two codirectionally-oriented carboxyl groups within the same covalent skeleton (like the *supramolecular* bis-carboxylic acids [BPP34C10·(2)₂]²⁺ and [BPP34C10·(3)₂]²⁺) can combine to form dimeric supermolecules in the solid state.^[5f,32] Likewise, *molecular* bis-isophthalic acids, wherein two isophthalic acid moieties are located at the opposite ends of a covalent framework, exhibit (like the corresponding *supramolecular* bis-isophthalic acid [BPP34C10·(6)₂]²⁺) the formation of supramolecular cross-linked polymers^[33] in the solid state.^[10c,24a] However, as we have demonstrated previously,^[7f] one should not underestimate the potential role of the PF₆[−] anions (and solvent molecules) in influencing these self-assembly processes.

Conclusions

The crystal structures considered in this paper illustrate a powerful synthetic supramolecular paradigm^[3] that may be employed for the rational noncovalent synthesis of interwoven supramolecular architectures in the solid state. More generally, they show that complex superstructures may be generated easily by using the concomitant self-selective^[7e] operation of several distinct recognition algorithms: in this instance, hydrogen-bonding motifs. In all the cases reported, the thread-like cations are inserted through the cavities of the macrocyclic polyethers with their NH₂⁺ centers interacting with the polyether loops, thus leaving their pendant carboxyl groups available for additional noncovalent association. For the most part, the recognition algorithms operate independently of one another, so that crossover does not usually occur between hydrogen-bonding motifs, that is, running the crown ether–dialkylammonium cation and carboxyl dimer supramolecular synthons simultaneously allows the creation of



Scheme 2. Cartoon highlighting the role of BPP34C10 as a girdle for supramolecular synthesis that, possibly in conjunction with attendant anions, dictates the orientation of recognition sites in space.

elaborate supramolecular aggregates and arrays. The idea that operating concurrently at least two orthogonal recognition algorithms simplifies noncovalent syntheses dramatically is one that is rapidly gaining credence amongst those working in synthetic supramolecular chemistry. Indeed, we and others had previously used the concurrent operation of combinations of disparate recognition algorithms, such as metal–ligand/hydrogen-bonding^[16] or π – π stacking/hydrogen-bonding^[7c, 15a, 15d] algorithms, for the solid-state supramolecular synthesis of interwoven superstructures that would once have been inconceivable. The research presented here demonstrates that a combination of two different algorithms of the same type (in this case, hydrogen-bonding interactions) can also be employed for the noncovalent synthesis of interwoven superstructures in the solid state. It must be emphasized, however, that only once the factors involved in crystal packing are completely understood will synthetic supramolecular chemists be able to control inter(supra)molecular architectures with a level of precision comparable to that which has been observed hitherto in natural systems.

Experimental Section

General: Flash chromatography was carried out employing the customary procedures.^[34] Melting points were determined on an Electrothermal 9200 melting point apparatus and are uncorrected. ¹H and ¹³C NMR spectra were recorded at 20 °C on a Bruker AC300 spectrometer (at 300.1 and 75.5 MHz, respectively) with the deuterated solvent as the lock and the residual solvent as internal reference. Liquid secondary ion mass spectra (LSIMS) were obtained from a VG ZabSpec mass spectrometer equipped with a cesium ion source and utilizing a *m*-nitrobenzyl alcohol matrix. Electron-impact mass spectra (EIMS) were obtained from a VG ProSpec mass spectrometer. Microanalyses were performed by the University of North London Microanalytical Services.

Benzyl-4-carboxybenzylammonium hexafluorophosphate (2·PF₆): A solution of benzylamine (**10**, 1.50 g, 14.0 mmol) and methyl 4-formylbenzoate (**7**, 2.30 g, 14.0 mmol) in PhMe (205 mL) was heated under reflux for 15.5 h while the H₂O discharged was isolated with a Dean–Stark separator. The solution was filtered while hot and the solvent evaporated off under reduced pressure to yield 3.53 g (100%) of 4-carbomethoxybenzylidenebenzylamine as a white solid [¹H NMR (CDCl₃): δ = 3.95 (s, 3H), 4.87 (s, 2H), 7.24–7.25 (m, 5H), 7.85 (d, *J* = 8 Hz, 2H), 8.09 (d, *J* = 8 Hz, 2H), 8.45 (s, 1H)], which was dissolved in a THF/MeOH solution (1:1, 110 mL). NaBH₄ (0.57 g, 15.0 mmol) was added with stirring at ambient temperature. A further portion of NaBH₄ (0.59 g, 15.5 mmol) was added to the reaction mixture after an additional 2 h. The solution was stirred subsequently for 20 h, before being treated with 1N HCl to adjust the pH to 2. After evaporation of the solvent in vacuo, the residue was partitioned between 1N NaOH (100 mL) and CH₂Cl₂ (100 mL). The aqueous phase was then further extracted with CH₂Cl₂ (2 × 100 mL). The combined organic extracts were dried (MgSO₄), filtered, and concentrated to afford 3.37 g (95%) of benzyl-4-carbomethoxybenzylamine **13**^[7e] as a pale brown oil [¹H NMR

(CDCl₃): δ = 3.79 (s, 2H), 3.85 (s, 2H), 3.89 (s, 3H), 7.15–7.37 (m, 5H), 7.41 (d, *J* = 8 Hz, 2H), 7.99 (d, *J* = 8 Hz, 2H)]. A portion of this aminoester (1.03 g, 4.0 mmol) was boiled with 12N HCl (40 mL) for 19 h. On cooling, the residual white solid was collected and washed with EtOH (25 mL), CHCl₃ (25 mL), and Et₂O (25 mL). The solid was taken up in boiling H₂O (300 mL), then a solution of NH₄PF₆ (0.86 g, 5.3 mmol) in H₂O (8 mL) was added and the cooled solution extracted with MeNO₂ (3 × 200 mL). The combined MeNO₂ extracts were washed with H₂O (200 mL) and the solvent evaporated off under reduced pressure to provide the title compound as a white solid (0.97 g, 62%). M.p. 176–179 °C; ¹H NMR (CD₃CN): δ = 4.25 (s, 2H), 4.29 (s, 2H), 7.46 (s, 5H), 7.57 (d, *J* = 8 Hz, 2H), 8.06 (d, *J* = 8 Hz, 2H); ¹³C NMR (CD₃CN): δ = 51.9, 52.8, 128.9, 130.2, 130.9, 131.25, 131.28, 131.32, 132.0, 136.6, 168.5; MS (LSI): *m/z* = 242 [*M* – PF₆]⁺; C₁₅H₁₆F₆NO₂P (387.3); calcd C 46.52, H 4.16, N 3.62; found C 46.41, H 4.16, N 3.53.

Benzyl-3-carboxybenzylammonium hexafluorophosphate (3·PF₆): Benzylamine (**10**, 1.61 g, 15.0 mmol) was condensed with methyl 3-formylbenzoate (**8**,^[35] 2.46 g, 15.0 mmol) following the general procedure (vide supra) to provide 3-carbomethoxybenzylidenebenzylamine (3.80 g, 100%) as an oily white solid [¹H NMR (CDCl₃): δ = 3.93 (s, 3H), 4.85 (s, 2H), 7.28–7.38 (m, 5H), 7.49 (t, *J* = 8 Hz, 1H), 8.02 (d, *J* = 8 Hz, 1H), 8.10 (d, *J* = 8 Hz, 1H), 8.39 (s, 1H), 8.43 (s, 1H)], which was reduced with NaBH₄ (see preparation of **13**) to furnish benzyl-3-carbomethoxybenzylamine (**14**, 3.83 g, 100%) as a yellow oil [¹H NMR (CDCl₃): δ = 3.81 (s, 2H), 3.85 (s, 2H), 3.91 (s, 3H), 7.22–7.44 (m, 6H), 7.56 (d, *J* = 8 Hz, 1H), 7.93 (d, *J* = 8 Hz, 1H), 8.02 (s, 1H)]. A portion of this aminoester (1.04 g, 4.1 mmol) was converted into the title compound by a procedure similar to that described for **2**·PF₆; a white solid (1.27 g, 80%) was obtained. M.p. 191–194 °C with decomp.; ¹H NMR (CD₃CN): δ = 4.25 (s, 2H), 4.31 (s, 2H), 7.46 (s, 5H), 7.58 (t, *J* = 8 Hz, 1H), 7.71 (d, *J* = 8 Hz, 1H), 8.07 (d, *J* = 8 Hz, 1H), 8.16 (s, 1H); ¹³C NMR (CD₃CN): δ = 52.1, 52.7, 129.7, 130.0, 130.2, 130.6, 131.0, 131.9, 132.0, 132.4, 132.7, 136.1, 167.3; MS (LSI): *m/z* = 242 [*M* – PF₆]⁺; C₁₅H₁₆F₆NO₂P (387.3); calcd C 46.52, H 4.16, N 3.62; found C 46.68, H 4.25, N 3.68.

Bis(4-carboxybenzyl)ammonium hexafluorophosphate (4·PF₆): Bis(4-carbomethoxybenzyl)amine (**15**,^[36] 0.52 g, 1.7 mmol) was transformed into the title compound by the general procedure given above for **2**·PF₆. It was acquired as a white solid (0.46 g, 65%). M.p. 209–213 °C; ¹H NMR (CD₃CN): δ = 4.31 (s, 4H), 7.56 (d, *J* = 8 Hz, 4H), 8.06 (d, *J* = 8 Hz, 4H); ¹³C NMR (CD₃CN): δ = 51.9, 131.0, 131.2, 132.1, 136.0, 167.3; MS (LSI): *m/z* = 286 [*M* – PF₆]⁺; C₁₆H₁₆F₆NO₄P (431.3); calcd C 44.56, H 3.74, N 3.25; found C 44.37, H 3.57, N 3.92.

Methyl 3-aminomethylbenzoate (12): HCl gas was bubbled through a solution of 3-carboxybenzylammonium chloride^[20] (2.48 g, 13.2 mmol) in MeOH (110 mL) for 10 min. The resultant solution was heated under reflux for 14 h with protection from the atmosphere. The solution was filtered and the solvent removed in vacuo. The residual white solid was triturated with Et₂O (140 mL) before being collected and partitioned between 5% aqueous Na₂CO₃ (40 mL) and CH₂Cl₂ (60 mL). The aqueous phase was further extracted with CH₂Cl₂ (3 × 60 mL), then the combined organic extracts were dried (MgSO₄), filtered, and concentrated to provide the title compound as a colorless oil (0.63 g, 29%). ¹H NMR (CDCl₃): δ = 1.54 (brs, 2H), 3.87 (s, 5H), 7.36 (t, *J* = 8 Hz, 1H), 7.47 (d, *J* = 8 Hz, 1H), 7.87 (d, *J* = 8 Hz, 1H), 7.95 (s, 1H); ¹³C NMR (CDCl₃): δ = 46.1, 52.1, 128.0, 128.1, 128.6, 130.3, 131.7, 143.6, 167.1; HRMS (EI) C₉H₁₂NO₂ [*M*+H]⁺: calcd *m/z* = 166.0868; found *m/z* = 166.0872.

Bis(3-carboxybenzyl)ammonium hexafluorophosphate (5·PF₆): Methyl 3-aminomethylbenzoate (**12**, 0.62 g, 3.8 mmol) was condensed with methyl 3-formylbenzoate (**8**,^[35] 0.62 g, 3.8 mmol) following the general procedure (vide supra) to provide 3-carbomethoxybenzylidene-3-carbomethoxybenzylamine as a viscous yellow oil (1.13 g, 97%) [¹H NMR (CDCl₃): δ = 3.91 (s, 3H), 3.93 (s, 3H), 4.88 (s, 2H), 7.41–7.61 (m, 3H), 7.93–8.14 (m, 4H), 8.40 (s, 1H), 8.46 (s, 1H)], which was reduced with NaBH₄ (see preparation of **13**) to provide bis(3-carbomethoxybenzyl)amine (**16**) as a thick yellow oil (1.02 g, 90%) [¹H NMR (CDCl₃): δ = 3.85 (s, 4H), 3.91 (s, 6H), 7.40 (t, *J* = 8 Hz, 2H), 7.55 (d, *J* = 8 Hz, 2H), 7.93 (d, *J* = 8 Hz, 2H), 8.01 (s, 2H)], which was boiled with a stirred 12N HCl solution (28 mL) for 68 h. The

reaction mixture was treated with H₂O (20 mL) and the precipitated solid collected. This solid was washed with H₂O (20 mL), Me₂CO (20 mL), and Et₂O (20 mL), before being suspended in Me₂CO (300 mL). 0.2 M NH₄PF₆ was added, and the suspension stirred at room temperature for 1 h. The resulting clear solution was filtered and the Me₂CO removed under reduced pressure so that the hexafluorophosphate salt precipitated out of solution. The suspension that remained was treated with H₂O (200 mL), the solid collected and then washed with H₂O. The solid was then dissolved in Me₂CO (200 mL), 30 mg of decolorizing charcoal was added, and the solution boiled for 5 min, before being filtered while hot. This procedure was repeated and the solvent was evaporated off under reduced pressure to provide **5**·PF₆ as a white solid (1.00 g, 71%). M.p. 217 °C with decomp.; ¹H NMR (CD₃CN): δ = 4.31 (s, 4H), 7.59 (t, *J* = 8 Hz, 2H), 7.69 (d, *J* = 8 Hz, 2H), 8.07 (d, *J* = 8 Hz, 2H), 8.13 (s, 2H); ¹³C NMR (CD₃CN): δ = 51.9, 130.3, 131.6, 131.7, 132.3, 133.6, 135.7, 166.0; MS (LSI): *m/z* = 286 [*M* – PF₆]⁺; C₁₆H₁₆F₆NO₄P (431.3): calcd C 44.56, H 3.74, N 3.25; found C 44.71, H 3.62, N 3.20.

Diethyl 5-formylisophthalate (9): A stirred solution of diethyl 5-bromo-methylisophthalate^[18] (1.26 g, 4.0 mmol) and bis(tetrabutylammonium) dichromate (5.62 g, 8.0 mmol) in CHCl₃ (20 mL) was heated under reflux for 2.5 h. On cooling to ambient temperature, the reaction mixture was filtered through 19.5 g of flash silica. The silica was washed with Et₂O (250 mL) and the combined CHCl₃ and Et₂O solutions concentrated to give a dark brown gum. Flash chromatography with CH₂Cl₂ provided the title compound as a white solid (0.76 g, 76%). M.p. 90 °C; ¹H NMR (CDCl₃): δ = 1.39 (t, *J* = 7 Hz, 6H), 4.40 (q, *J* = 7 Hz, 4H), 8.65 (s, 2H), 8.85 (s, 1H), 10.09 (s, 1H); ¹³C NMR (CDCl₃): δ = 14.3, 61.9, 132.2, 134.2, 135.7, 136.8, 164.8, 190.6; MS (EI): *m/z* = 250 [*M*]⁺; C₁₃H₁₄O₅ (250.3): calcd C 62.39, H 5.64; found C 62.57, H 5.54.

Benzyl-3,5-dicarboxybenzylammonium hexafluorophosphate (6·PF₆): Following the standard procedure (vide supra), benzylamine (**10**, 0.32 g, 3.0 mmol) was condensed with diethyl 5-formylisophthalate (**9**, 0.74 g, 3.0 mmol) to give 3,5-dicarboethoxybenzylidenebenzylamine as a white solid (0.98 g, 97%) [¹H NMR (CDCl₃): δ = 1.40 (t, *J* = 7 Hz, 6H), 4.41 (q, *J* = 7 Hz, 4H), 4.88 (s, 2H), 7.10–7.43 (m, 5H), 8.46 (s, 2H), 8.59 (s, 1H), 8.72 (s, 1H)]. A portion of this aldimine (0.21 g, 0.6 mmol) was reduced with NaBH₄ (see preparation of **13**) to afford benzyl-3,5-dicarboethoxybenzylamine **17** as a yellow oil (0.20 g, 95%) [¹H NMR (CDCl₃): δ = 1.38 (t, *J* = 7 Hz, 6H), 3.78 (s, 2H), 3.86 (s, 2H), 4.37 (q, *J* = 7 Hz, 4H), 7.19–7.39 (m, 5H), 8.19 (s, 2H), 8.54 (s, 1H)], that was transformed into the title compound **6**·PF₆ (employing a procedure similar to that described for **2**·PF₆), which was obtained as a white solid (0.15 g, 59%). M.p. 194–195 °C with decomp.; ¹H NMR (CD₃CN): δ = 4.25 (s, 2H), 4.38 (s, 2H), 7.46 (s,

5H), 8.35 (s, 2H), 8.58 (s, 1H); ¹³C NMR (CD₃CN): δ = 51.4, 52.5, 130.0, 130.5, 130.7, 131.0, 131.8, 132.2, 132.4, 136.7, 166.3; MS (LSI): *m/z* = 286 [*M* – PF₆]⁺; C₁₆H₁₆F₆NO₄P (431.3): calcd C 44.56, H 3.74, N 3.25; found C 44.49, H 3.95, N 3.17.

Crystal growth: The crystal growing methods that were used have been described by Jones.^[37] Table 4 lists the techniques employed and the solvent systems utilized for the preparation of single crystals that were suitable for X-ray crystallographic analysis.

X-ray crystallography: Table 5 provides a summary of the crystal data, data collection and refinement parameters for complexes [DB24C8·**2**][PF₆], [DB24C8·**4**][PF₆], [DB24C8·**5**][PF₆], [DB24C8·**6**][PF₆], [BPP34C10·(2)₂][PF₆]₂, [BPP34C10·(3)₂][PF₆]₂ and [BPP34C10·(6)₂][PF₆]₂. Although structure solution and refinement details for [BPP34C10·(2)₂][PF₆]₂ and [BPP34C10·(6)₂][PF₆]₂ have already been published,^[17] the data for these compounds are included here as their structures have been refined again slightly differently. The structures were solved by direct methods and were refined by full-matrix least-squares based on *F*². In [DB24C8·**5**][PF₆] and [BPP34C10·(6)₂][PF₆]₂, disorder was found in part of one of the polyether linkages and, in the latter, in the benzyl ring of the cation. In each case, this disorder was resolved into two partial-occupancy orientations, the major occupancy portions of which were refined anisotropically. In [DB24C8·**2**][PF₆], [DB24C8·**4**][PF₆], [DB24C8·**6**][PF₆], and [BPP34C10·(6)₂][PF₆]₂, the PF₆[−] anions were found to be disordered. For each structure, this disorder was resolved into two partial-occupancy orientations, the major occupancy portions of which were refined anisotropically. The PhH solvent molecules in [DB24C8·**2**][PF₆] were optimized and refined anisotropically. The included Me₂CO molecules in [DB24C8·**4**][PF₆] were ordered and refined anisotropically. The solvent molecules in [DB24C8·**5**][PF₆] were found to be disordered over two partial-occupancy sites, the atoms of both being refined isotropically. In [DB24C8·**6**][PF₆], the half-occupancy included Me₂CO molecule was refined anisotropically. The MeCN molecules in [BPP34C10·(2)₂][PF₆]₂ were not clearly defined, and the solvent was modeled by the assignment of various peaks of electron density to total up to two-and-a-half molecules. In [BPP34C10·(3)₂][PF₆]₂, the three included PhH molecules were found to be a mixture of ordered and disordered molecules (with two of the ordered ones positioned about centers of symmetry), all the non-hydrogen atoms of which were refined anisotropically. In [BPP34C10·(6)₂][PF₆]₂, the two PhH molecules were found to be distributed over three partial occupancy sites, all of which were refined isotropically. The remaining non-hydrogen atoms in all of the structures were refined anisotropically. In each structure, the C–H hydrogen atoms were placed in calculated positions, assigned isotropic thermal parameters, *U*(H) = 1.2*U*_{eq}(C) [*U*(H) = 1.5*U*_{eq}(C–Me)], and allowed to ride on their parent atoms. The N–H hydrogen atoms in all the structures were optimized and refined isotropically. In [DB24C8·**2**][PF₆], [DB24C8·**4**][PF₆], and [DB24C8·**6**][PF₆] the O–H hydrogen atoms were located from Δ*F* maps and refined isotropically—in the other four structures, these hydrogen atoms could not be located. Computations were carried out using the SHELXTL PC program system.^[38] Crystallographic data (excluding structure factors) for the structures reported in this paper have been deposited with the Cambridge Crystallographic Data Centre as supplementary publication no. CCDC-100689. Copies of the data can be obtained free of charge on application to CCDC, 12 Union Road, Cambridge CB21EZ, UK (Fax: (+ 44) 1223-336-033; e-mail: deposit@ccdc.cam.ac.uk).

Table 4. Solvents and methods employed for the crystallization of the pseudorotaxane complexes reported in this paper.

	Solvent ^[c]	Precipitant ^[d]	Method
[DB24C8· 2][PF ₆] ^[a]	MeNO ₂	PhH	liquid diffusion ^[e]
[DB24C8· 4][PF ₆] ^[a]	Me ₂ CO	<i>i</i> Pr ₂ O	liquid diffusion ^[e]
[DB24C8· 5][PF ₆] ^[a]	Me ₂ CO	<i>i</i> Pr ₂ O	liquid diffusion ^[e]
[DB24C8· 6][PF ₆] ^[a]	Me ₂ CO	<i>n</i> C ₆ H ₁₄	liquid diffusion ^[e]
[BPP34C10·(2) ₂][PF ₆] ^[b]	MeCN/(ClCH ₂) ₂	<i>i</i> Pr ₂ O	liquid diffusion ^[e]
[BPP34C10·(3) ₂][PF ₆] ^[b]	Me ₂ CO	PhH	slow evaporation ^[f]
[BPP34C10·(6) ₂][PF ₆] ^[b]	Me ₂ CO	PhH	slow evaporation ^[f]

[a] Crystals were obtained from a solution containing equimolar amounts of the pseudorotaxane constituents. [b] Crystals were acquired from a solution containing a 1:2 molar ratio of BPP34C10 and the appropriate ammonium salt. [c] Good solvent in which the pseudorotaxane complexes are soluble. [d] Poor solvent in which the pseudorotaxane complexes are insoluble. [e] In the *liquid diffusion* method, the pseudorotaxanes' constituents were dissolved in a small amount of solvent, then the precipitant was carefully layered on top of the resulting solution. X-ray quality single crystals were obtained after several days, when the precipitant had diffused totally into the solution. [f] In the *slow evaporation* method, the pseudorotaxane components were dissolved in a small amount of solvent. The solution was mixed thoroughly with an amount of precipitant that did not induce immediate crystallization, then the solution was allowed to slowly evaporate at 20 °C over several days, resulting in the formation of single crystals that were suitable for X-ray crystallographic analysis.

Acknowledgments: This research was sponsored by an Engineering and Physical Sciences Research Council CASE Award (to M.C.T.F.) and the Biotechnology and Biological Sciences Research Council.

Received: September 11, 1997 [F818]

- [1] a) M. Mascal, *Contemp. Org. Synth.* **1994**, *1*, 31–46; b) J.-M. Lehn, *Supramolecular Chemistry*, VCH, Weinheim, **1995**.
- [2] For some recent examples, see: a) M. Fujita, D. Oguro, M. Miyazawa, H. Oka, K. Yamaguchi, K. Ogura, *Nature (London)* **1995**, *378*, 469–471; b) J. D. Hartgerink, J. R. Granja, R. A. Milligan, M. R. Ghadiri, *J. Am. Chem. Soc.* **1996**, *118*, 43–50; c) R. W. Saalfrank, N. Low, F. Hampel, H. D. Stachel, *Angew. Chem.* **1996**, *108*, 2353–2354; *Angew. Chem. Int. Ed. Engl.* **1996**, *35*, 2209–2210; d) J. A. R. P. Sarma, F. H. Allen, V. J. Hoy, J. A. K. Howard, R. Thaimattam, K. Biradha, G. R.

Table 5. Crystal data, data collection, and refinement parameters.^[a]

	[DB24C8·2]- [PF ₆]	[DB24C8·4]- [PF ₆]	[DB24C8·5]- [PF ₆]	[DB24C8·6]- [PF ₆]	[BPP34C10·(2) ₂]- [PF ₆] ₂	[BPP34C10·(3) ₂]- [PF ₆] ₂	[BPP34C10·(6) ₂]- [PF ₆] ₂
formula	C ₃₉ H ₄₈ NO ₁₀ ·PF ₆	C ₄₀ H ₄₈ NO ₁₂ ·PF ₆	C ₄₀ H ₄₈ NO ₁₂ ·PF ₆	C ₄₀ H ₄₈ NO ₁₂ ·PF ₆	C ₅₈ H ₇₂ N ₂ O ₁₄ ·2PF ₆	C ₅₈ H ₇₂ N ₂ O ₁₄ ·2PF ₆	C ₆₀ H ₇₂ N ₂ O ₁₈ ·2PF ₆
solvent	2 PhH	Me ₂ CO	0.25 Me ₂ CO	0.5 Me ₂ CO	2.5 MeCN	3 PhH	2 PhH
formula weight	992.0	937.8	894.3	908.8	1413.8	1545.4	1555.4
color, habit	clear blocks	clear prisms	clear prismatic needles	clear prisms	clear plates	clear plates	clear rhombs
crystal size (mm)	0.83 × 0.83 × 0.67	0.93 × 0.83 × 0.40	0.50 × 0.30 × 0.13	0.53 × 0.50 × 0.40	0.37 × 0.33 × 0.30	0.83 × 0.63 × 0.10	0.30 × 0.28 × 0.10
lattice type	monoclinic	triclinic	triclinic	monoclinic	triclinic	triclinic	monoclinic
space group	<i>P</i> 2 ₁ / <i>c</i> , 14	<i>P</i> 1̄, 2	<i>P</i> 1̄, 2	<i>P</i> 2 ₁ / <i>n</i> , 14	<i>P</i> 1̄, 2	<i>P</i> 2 ₁ / <i>c</i> , 14	<i>P</i> 2 ₁ / <i>c</i> , 14
<i>T</i> (K)	293	293	293	293	293	203	293
<i>a</i> (Å)	16.248(3)	11.908(1)	11.015(3)	16.890(1)	10.619(1)	10.154(1)	12.513(1)
<i>b</i> (Å)	17.194(3)	12.336(1)	11.022(1)	15.997(2)	17.292(1)	17.209(1)	16.555(1)
<i>c</i> (Å)	19.002(3)	16.627(2)	19.764(2)	20.949(1)	22.109(2)	24.643(5)	18.593(1)
<i>α</i> (°)	–	79.92(1)	78.39(1)	–	79.64(1)	105.49(1)	–
<i>β</i> (°)	105.99(1)	83.55(1)	77.94(2)	104.79(1)	79.54(1)	101.51(2)	96.10(1)
<i>γ</i> (°)	–	76.17(1)	89.81(1)	–	76.94(1)	99.27(1)	–
<i>V</i> (Å ³)	5103(1)	2328.8(4)	2296.6(7)	5472.7(9)	3848.2(4)	3960.1(9)	3829.7(5)
<i>Z</i>	4	2	2	4	2	2	2 ^[b]
<i>ρ</i> _{calcd} (g cm ⁻³)	1.291	1.337	1.293	1.103	1.220	1.296	1.349
<i>F</i> (000)	2088	984	936	1904	1478	1620	1624
radiation used	MoK _α	MoK _α	CuK _α	CuK _α ^[c]	CuK _α ^[c]	CuK _α ^[c]	CuK _α ^[c]
<i>μ</i> (mm ⁻¹)	0.13	0.15	1.26	1.07	1.27	1.27	1.36
<i>θ</i> range	1.8–22.5	2.0–25.0	2.3–63.0	3.0–57.5	2.0–55.0	1.9–55.0	3.6–60.0
no. unique reflns measured	6625	8157	7400	7421	7886	9776	5661
no. unique reflns observed,	3994	4844	5257	3566	3167	5485	3497
<i>F</i> _o > 4σ(<i>F</i> _o)							
no. of variables	594	622	586	614	813	933	550
<i>R</i> ₁ ^[d]	0.063	0.079	0.083	0.130	0.158	0.090	0.087
<i>wR</i> ₂ ^[e]	0.164	0.217	0.246	0.337	0.401	0.212	0.237
weighting factors	0.086, 4.589	0.126, 1.334	0.170, 0.713	0.249, 0.000	0.326, 5.190	0.110, 7.276	0.139, 3.740
<i>a</i> , <i>b</i> ^[f]							
largest difference peak, hole (e Å ⁻³)	0.33, –0.25	0.50, –0.42	0.65, –0.29	0.89, –0.35	0.89, –0.49	0.53, –0.31	0.40, –0.39

[a] Details in common: graphite-monochromated radiation, *ω*-scans, Siemens P4 diffractometer, refinement based on *F*². [b] The supermolecule has crystallographic C₃ symmetry. [c] Rotating anode source. [d] $R_1 = \sum ||F_o| - |F_c|| / \sum |F_o|$. [e] $wR_2 = \sqrt{[\sum w(F_o^2 - F_c^2)^2] / \sum w(F_o^2)}$. [f] $w^{-1} = \sigma^2(F_o^2) + (aP)^2 + bP$.

- Desiraju, *Chem. Commun.* **1997**, 101–102; e) J. A. Whiteford, C. V. Lu, P. J. Stang, *J. Am. Chem. Soc.* **1997**, *119*, 2524–2533; f) T. L. Hennigar, D. C. MacQuarrie, P. Losier, R. D. Rogers, M. J. Zaworotko, *Angew. Chem.* **1997**, *109*, 1044–1046; *Angew. Chem. Int. Ed. Engl.* **1997**, *36*, 972–973; g) D. P. Funeriu, J.-M. Lehn, G. Baum, D. Fenske, *Chem. Eur. J.* **1997**, *3*, 99–104; h) D. L. Caulder, K. N. Raymond, *Angew. Chem.* **1997**, *109*, 1508–1510; *Angew. Chem. Int. Ed. Engl.* **1997**, *36*, 1440–1442.
- [3] M. C. T. Fyfe, J. F. Stoddart, *Acc. Chem. Res.* **1997**, *30*, 393–401.
- [4] J. R. Fredericks, A. D. Hamilton in *Comprehensive Supramolecular Chemistry*, Vol. 9 (Eds.: J. L. Atwood, J. E. D. Davies, D. D. MacNicol, F. Vögtle), Pergamon, Oxford, **1996**, pp. 565–594.
- [5] For some recent examples, see: a) J. A. Zerkowski, C. T. Seto, G. M. Whitesides, *J. Am. Chem. Soc.* **1992**, *114*, 5473–5475; b) S. C. Zimmerman, B. F. Duerr, *J. Org. Chem.* **1992**, *57*, 2215–2217; c) J. Yang, E. Fan, S. J. Geib, A. D. Hamilton, *J. Am. Chem. Soc.* **1993**, *115*, 5314–5315; d) M. Mascal, N. M. Hext, R. Warmuth, M. H. Moore, J. P. Turkenburg, *Angew. Chem.* **1996**, *108*, 2347–2350; *Angew. Chem. Int. Ed. Engl.* **1996**, *35*, 2204–2206; e) C. M. Drain, K. C. Russell, J.-M. Lehn, *Chem. Commun.* **1996**, 337–338; f) O. Struck, W. Verboom, W. J. J. Smeets, A. L. Spek, D. N. Reinhoudt, *J. Chem. Soc. Perkin Trans. 2* **1997**, 223–227; g) R. Meissner, X. Garcias, S. Mecozzi, J. Rebek, Jr., *J. Am. Chem. Soc.* **1997**, *119*, 77–85; h) R. F. M. Lange, F. H. Beijer, R. P. Sijbesma, R. W. W. Hoof, H. Kooijman, A. L. Spek, J. Kroon, E. W. Meijer, *Angew. Chem.* **1997**, *109*, 1006–1008; *Angew. Chem. Int. Ed. Engl.* **1997**, *36*, 969–971; i) E. E. Simanek, S. Qiao, I. S. Choi, G. M. Whitesides, *J. Org. Chem.* **1997**, *62*, 2619–2621; j) M. C. Feiters, M. C. T. Fyfe, M. V. Martínez-Díaz, S. Menzer, R. J. M. Nolte, J. F. Stoddart, P. J. M. van Kan, D. J. Williams, *J. Am. Chem. Soc.* **1997**, *119*, 8119–8120; k) K. D. M. Harris, B. M. Kariuki, C. Lambropoulos, D. Philp, J. M. A. Robinson, *Tetrahedron* **1997**, *53*, 8599–8612.
- [6] For some recent examples, see: a) S. Hanessian, M. Simard, S. Roelens, *J. Am. Chem. Soc.* **1995**, *117*, 7630–7645; b) P. R. Ashton, G. R. Brown, W. Hayes, S. Menzer, D. Philp, J. F. Stoddart, D. J. Williams, *Adv. Mater.* **1996**, *8*, 564–567; c) K. E. Schwiebert, D. N. Chin, J. C. MacDonald, G. M. Whitesides, *J. Am. Chem. Soc.* **1996**, *118*, 4018–4029; d) R. E. Melendez, C. V. K. Sharma, M. J. Zaworotko, C. Bauer, R. D. Rogers, *Angew. Chem.* **1996**, *108*, 2357–2359; *Angew. Chem. Int. Ed. Engl.* **1996**, *35*, 2213–2215; e) C. B. Aakeröy, D. P. Hughes, M. Niewenhuyzen, *J. Am. Chem. Soc.* **1996**, *118*, 10134–10140; f) C. V. K. Sharma, M. J. Zaworotko, *Chem. Commun.* **1996**, 2655–2656; g) O. Félix, M. W. Hosseini, A. De Cian, J. Fischer, *Angew. Chem.* **1997**, *109*, 134–136; *Angew. Chem. Int. Ed. Engl.* **1997**, *36*, 102–104; h) K. Endo, T. Ezuhara, M. Koyanagi, H. Masuda, Y. Aoyama, *J. Am. Chem. Soc.* **1997**, *119*, 499–505; i) K. R. Adam, I. M. Atkinson, R. L. Davis, L. F. Lindoy, M. S. Mahinay, B. J. McCool, B. W. Skelton, A. H. White, *Chem. Commun.* **1997**, 467–468; j) P. Brunet, M. Simard, J. D. Wuest, *J. Am. Chem. Soc.* **1997**, *119*, 2737–2738; k) V. A. Russell, C. C. Evans, W. Li, M. D. Ward, *Science* **1997**, *276*, 575–579; l) I. L. Karle, D. Ranganathan, V. Haridas, *J. Am. Chem. Soc.* **1997**, *119*, 2777–2783.
- [7] a) P. R. Ashton, P. J. Campbell, E. J. T. Chrystal, P. T. Glink, S. Menzer, D. Philp, N. Spencer, J. F. Stoddart, P. A. Tasker, D. J. Williams, *Angew. Chem.* **1995**, *107*, 1997–2001; *Angew. Chem. Int. Ed. Engl.* **1995**, *34*, 1865–1869; b) P. R. Ashton, E. J. T. Chrystal, P. T. Glink, S. Menzer, C. Schiavo, J. F. Stoddart, P. A. Tasker, D. J. Williams, *ibid.* **1995**, *107*, 2001–2004 and *34*, 1869–1871; c) P. R. Ashton, E. J. T. Chrystal, P. T. Glink, S. Menzer, C. Schiavo, N.

- Spencer, J. F. Stoddart, P. A. Tasker, A. J. P. White, D. J. Williams, *Chem. Eur. J.* **1996**, *2*, 709–728; d) P. T. Glink, C. Schiavo, J. F. Stoddart, D. J. Williams, *Chem. Commun.* **1996**, 1483–1490; e) P. R. Ashton, P. T. Glink, M.-V. Martínez-Díaz, J. F. Stoddart, A. J. P. White, D. J. Williams, *Angew. Chem.* **1996**, *108*, 2058–2061; *Angew. Chem. Int. Ed. Engl.* **1996**, *35*, 1930–1933; f) M. C. T. Fyfe, P. T. Glink, S. Menzer, J. F. Stoddart, A. J. P. White, D. J. Williams, *ibid.* **1997**, *109*, 2158–2160 and *36*, 2068–2070; g) P. R. Ashton, M. C. T. Fyfe, P. T. Glink, S. Menzer, J. F. Stoddart, A. J. P. White, D. J. Williams, *J. Am. Chem. Soc.* **1997**, *119*, 12514–12524.
- [8] a) D. S. Lawrence, T. Jiang, M. Levett, *Chem. Rev.* **1995**, *95*, 2229–2260; b) D. Philp, J. F. Stoddart, *Angew. Chem.* **1996**, *108*, 1242–1286; *Angew. Chem. Int. Ed. Engl.* **1996**, *35*, 1154–1196.
- [9] Pseudorotaxanes are *supramolecular* entities in which one or more thread-like species interpenetrate the cavities of one or more macrorings to generate inclusion complexes. Notably, as distinct from their mechanically-interlocked, *molecular* counterparts, the rotaxanes, pseudorotaxane supermolecules can dissociate into their individual components since they do not possess bulky stopper groups. For instance, see: a) P. R. Ashton, D. Philp, N. Spencer, J. F. Stoddart, *J. Chem. Soc. Chem. Commun.* **1991**, 1677–1679; b) P.-L. Anelli, P. R. Ashton, A. M. Z. Slawin, N. Spencer, J. F. Stoddart, D. J. Williams, *Angew. Chem.* **1991**, *103*, 1052–1054; *Angew. Chem. Int. Ed. Engl.* **1991**, *30*, 1036–1039; c) D. B. Amabilino, P.-L. Anelli, P. R. Ashton, G. R. Brown, E. Córdova, L. A. Godínez, W. Hayes, A. E. Kaifer, D. Philp, A. M. Z. Slawin, N. Spencer, J. F. Stoddart, M. S. Tolley, D. J. Williams, *J. Am. Chem. Soc.* **1995**, *117*, 11 142–11 170; d) P. R. Ashton, S. J. Langford, N. Spencer, J. F. Stoddart, A. J. P. White, D. J. Williams, *Chem. Commun.* **1996**, 1387–1388; e) P. N. W. Baxter, H. Sleiman, J.-M. Lehn, K. Rissanen, *Angew. Chem.* **1997**, *36*, 1350–1352; *Angew. Chem. Int. Ed. Engl.* **1997**, *36*, 1294–1296; f) A. Mirzozian, A. E. Kaifer, *Chem. Eur. J.* **1997**, *3*, 1052–1058.
- [10] a) L. Leiserowitz, *Acta Crystallogr. Sect. B* **1976**, *32*, 775–802; b) Z. Berkovitch-Yellin, L. Leiserowitz, *J. Am. Chem. Soc.* **1982**, *104*, 4052–4064; c) S. V. Kolotuchin, E. E. Fenlon, S. R. Wilson, C. J. Loweth, S. C. Zimmerman, *Angew. Chem.* **1995**, *107*, 2873–2876; *Angew. Chem. Int. Ed. Engl.* **1995**, *34*, 2654–2657 and references therein.
- [11] a) J. C. MacDonald, G. M. Whitesides, *Chem. Rev.* **1994**, *94*, 2383–2420; b) G. R. Desiraju, *Angew. Chem.* **1995**, *107*, 2541–2558; *Angew. Chem. Int. Ed. Engl.* **1995**, *34*, 2311–2327; c) *Comprehensive Supramolecular Chemistry*, Vol. 6 (Eds.: J. L. Atwood, J. E. D. Davies, D. D. MacNicol, F. Vögtle), Pergamon, Oxford, **1996**; d) V. A. Russell, M. D. Ward, *Chem. Mater.* **1996**, *8*, 1654–1666; e) G. R. Desiraju, *Chem. Commun.* **1997**, 1475–1482.
- [12] M. Bailey, C. J. Brown, *Acta Crystallogr.* **1967**, *22*, 387–391.
- [13] R. Alcalá, S. Martínez-Carrera, *Acta Crystallogr. Sect. B* **1972**, *28*, 1671–1677.
- [14] a) J. Yang, J. L. Marendez, S. J. Geib, A. D. Hamilton, *Tetrahedron Lett.* **1994**, *35*, 3665–3668; b) S. Valiyaveetil, V. Enkelmann, G. Moessner, K. Müllen, *Macromol. Symp.* **1996**, *102*, 165–173; c) S. C. Zimmerman, F. Zeng, D. E. C. Reichert, S. V. Kolotuchin, *Science* **1996**, *271*, 1095–1098.
- [15] a) M. Asakawa, P. R. Ashton, G. R. Brown, W. Hayes, S. Menzer, J. F. Stoddart, A. J. P. White, D. J. Williams, *Adv. Mater.* **1996**, *8*, 37–41; b) P. R. Ashton, R. Ballardini, V. Balzani, M. Belohradsky, M. T. Gandolfi, D. Philp, L. Prodi, F. M. Raymo, M. V. Reddington, N. Spencer, J. F. Stoddart, M. Venturi, D. J. Williams, *J. Am. Chem. Soc.* **1996**, *118*, 4931–4951; c) F. M. Raymo, J. F. Stoddart, *Trends Polym. Sci.* **1996**, *4*, 208–211; d) M. Asakawa, P. R. Ashton, C. L. Brown, M. C. T. Fyfe, S. Menzer, D. Pasini, C. Scheuer, N. Spencer, J. F. Stoddart, A. J. P. White, D. J. Williams, *Chem. Eur. J.* **1997**, *3*, 1136–1150.
- [16] Kim and his associates have employed coordinate covalent bonds between ligands and metals to link pseudorotaxanes in order to form interwoven supramolecular arrays. See: a) D. Whang, Y.-M. Jeon, J. Heo, K. Kim, *J. Am. Chem. Soc.* **1996**, *118*, 11 333–11 334; b) D. Whang, K. Kim, *ibid.* **1997**, *119*, 451–452.
- [17] A small part of this research has been reported in a communication. See: P. R. Ashton, A. N. Collins, M. C. T. Fyfe, S. Menzer, J. F. Stoddart, D. J. Williams, *Angew. Chem.* **1997**, *109*, 760–763; *Angew. Chem. Int. Ed. Engl.* **1997**, *36*, 735–739.
- [18] We prepared this compound employing the synthetic procedure that was first utilized by Collman and his associates. See: J. P. Collman, X. Zhang, K. Wang, J. I. Brauman, *J. Am. Chem. Soc.* **1994**, *116*, 6245–6251. However, this compound has been prepared more recently by Fréchet's group on a much larger scale. See: J. W. Leon, M. Kawa, J. M. J. Fréchet, *J. Am. Chem. Soc.* **1996**, *118*, 8847–8859.
- [19] a) D. Landini, F. Rolla, *Chem. Ind. (London)* **1979**, 213; b) G. A. Kraus, M. E. Krolski, *J. Org. Chem.* **1986**, *51*, 3347–3350; c) G. Mehta, S. R. Shah, Y. Venkateswarlu, *Tetrahedron* **1994**, *50*, 11 729–11 742.
- [20] S. Jackson, W. DeGrado, A. Dwivedi, A. Parthasarathy, A. Higley, J. Krywko, A. Rockwell, J. Markwalder, G. Wells, R. Wexler, S. Mousa, R. Harlow, *J. Am. Chem. Soc.* **1994**, *116*, 3220–3230.
- [21] a) R. C. Helgeson, T. L. Tarnowski, J. M. Timko, D. J. Cram, *J. Am. Chem. Soc.* **1977**, *99*, 6411–6418; b) H. W. Gibson, S. Liu, P. Lecavalier, C. Wu, Y. X. Shen, *ibid.* **1995**, *117*, 852–874. See also: c) Y. Delaviz, H. W. Gibson, *Polym. Commun.* **1991**, *32*, 103–105; d) Y. Delaviz, Y. X. Shen, H. W. Gibson, *Polymer* **1992**, *33*, 212–213.
- [22] However, when the peaks for the [DB24C8·cation]⁺ complexes were calibrated against peaks for the bis(4-*t*-butylbenzyl)ammonium cation (a cation that has been shown not to form complexes with DB24C8; P. R. Ashton, I. Baxter, M. C. T. Fyfe, F. M. Raymo, N. Spencer, J. F. Stoddart, A. J. P. White, D. J. Williams, *J. Am. Chem. Soc.* **1998**, *120*, 2297–2309), there appeared to be no clear relationship between the relative intensities of the peaks associated with the complexes and the *K_a* values obtained in solution.
- [23] However, in this instance, the signals are time-averaged, since the relatively large cavity of BPP34C10 allows fast association and dissociation of the components on the ¹H NMR time scale at 20 °C.
- [24] The disruption of noncovalent association between carboxyl groups by competitive polar solvents has been noted previously by researchers from other laboratories. See: a) A. Zafar, J. Yang, S. J. Geib, A. D. Hamilton, *Tetrahedron Lett.* **1996**, *37*, 2327–2330; b) Ref. [14c]. Unfortunately, the salts were barely soluble in CD₂Cl₂ alone, even in the presence of the crown ethers, thus precluding a study of carboxyl group association and, hence, interpseudorotaxane interactions in solution.
- [25] D. B. Amabilino, I. W. Parsons, J. F. Stoddart, *Trends Polym. Sci.* **1994**, *2*, 146–152.
- [26] I. R. Hanson, D. L. Hughes, M. R. Truter, *J. Chem. Soc. Perkin Trans. 2* **1976**, 972–978.
- [27] We have introduced the term co-conformation recently^[7f] to define the three-dimensional spatial arrangement of the atoms in supramolecular systems.
- [28] Swager and his associates have recently prepared side-chain pseudopolyrotaxanes possessing covalently linked polymeric backbones. See: a) M. J. Marsella, P. J. Carroll, T. M. Swager, *J. Am. Chem. Soc.* **1995**, *117*, 9832–9841; b) Q. Zhou, T. M. Swager, *ibid.* **1995**, *117*, 12 593–12 602.
- [29] Following this discovery, we reexamined the crystal structure^[7b,c] of the 2:2 [4]pseudorotaxane complex formed between α,α'-bis(benzylammonium)-*p*-xylene bis(hexafluorophosphate) and BPP34C10, where we found that one of the principal F–P–F axes of a PF₆⁻ anion was directed into the central cleft of the complex between two NH₂⁺ cationic centers. The contact distances from the hydrogen atoms of the [4]pseudorotaxane to either of these axial fluorine atoms are all greater than 2.8 Å. Nevertheless, a contact of ca. 2.5 Å was identified between one of the benzylic hydrogen atoms of the [4]pseudorotaxane and one of the equatorial fluorine atoms of the PF₆⁻ anion.
- [30] J.-M. Lehn, *Makromol. Chem. Macromol. Symp.* **1993**, *69*, 1–17.
- [31] a) D. J. Cram, *Angew. Chem.* **1986**, *98*, 1041–1060; *Angew. Chem. Int. Ed. Engl.* **1986**, *25*, 1039–1057; b) D. J. Cram, *ibid.* **1988**, *100*, 1041–1052, and *27*, 1009–1020.
- [32] For instance, see: a) F. Takusagawa, T. F. Koetzle, *Acta Crystallogr. Sect. B* **1979**, *35*, 2888–2896; b) L. J. Fitzgerald, J. C. Gallucci, R. E. Gerkin, *Acta Crystallogr. Sect. B* **1991**, *47*, 776–782; c) H. Díaz, K. Y. Tsang, D. Choo, J. W. Kelly, *Tetrahedron* **1993**, *49*, 3533–3545.
- [33] Note, however, that the cross-linking component of these supramolecular polymers is entirely covalent.
- [34] W. C. Still, M. Kahn, A. Mitra, *J. Org. Chem.* **1978**, *43*, 2923–2925.
- [35] H. Simonis, *Chem. Ber.* **1912**, *45*, 1584–1592.
- [36] P. R. Ashton, P. T. Glink, J. F. Stoddart, P. A. Tasker, A. J. P. White, D. J. Williams, *Chem. Eur. J.* **1996**, *2*, 729–736.
- [37] P. G. Jones, *Chem. Br.* **1981**, *17*, 222–225.
- [38] SHELXTL PC v. 5.03, Siemens Analytical X-Ray Instruments, Madison (WI), **1994**.